

# Quantification of metabolites of kinureninergic pathway and inflammatory biomarkers in biological samples of cardiac patients with heart failure: an exploratory pilot study

Ana Catarina Pinto de Sousa

Dissertation for the Degree of Master in Forensic Sciences and  
Laboratory Techniques

Gandra, October 2020



Ana Catarina Pinto de Sousa

Dissertation for the Degree of Master in Forensic Laboratory  
Science and Techniques of the University Institute of Health  
Sciences (IUCS, CESPU)

**Quantification of metabolites of kinureninergic pathway  
and inflammatory biomarkers in biological samples of  
cardiac patients with heart failure: an exploratory pilot  
study**

Under guidance of Professor Doctor Sandra Leal and Professor Doctor Cláudia Ribeiro.

## DECLARAÇÃO DE INTEGRIDADE

ANA CATARINA PINTO DE SOUSA, estudante do MESTRADO EM CIÊNCIAS E TÉCNICAS LABORATORIAIS FORENSES do Instituto Universitário de Ciências da Saúde, declaro ter atuado com absoluta integridade na elaboração desta Dissertação.

Confirmo que em todo o trabalho conducente à sua elaboração não recorri a qualquer forma de falsificação de resultados ou à prática de plágio (ato pelo qual um indivíduo, mesmo por omissão, assume a autoria do trabalho intelectual pertencente a outrem, na sua totalidade ou em partes dele).

Mais declaro que todas as frases que retirei de trabalhos anteriores pertencentes a outros autores foram referenciadas ou redigidas com novas palavras, tendo neste caso colocado a citação da fonte bibliográfica.

## ACKNOWLEDGMENT

I could not pass up the opportunity to thank some people who have been very important throughout these two years.

I would first like to thank Professor Doctor Sandra Leal who gave me the opportunity to have such an interesting and ambitious project as a dissertation topic. I would also like to thank her for all her support during these months.

Thank you to Professor Doctor Cláudia Ribeiro for all the help. She never gave up on me with all the difficulties throughout the development of the method and at the time of writing.

To the technique Virgínia Gonçalves, who has always been presented to help me in all the small big details of the equipment and during the validation process.

To teacher Joana Barbosa who patiently helped me to handle the self-analyzer.

I would also like to thank all the laboratory technicians and the co-workers who made this my second home.

To all my friends, a thank you is not enough. Even without understanding a word about the subject of the dissertation they read, encouraged and showed the greatest pride in the world.

Eternal gratitude to my parents who gave me all the support, support and care in moments that were not always easy and provided me with all the tools to finish this work successfully.

Last but not least, to my boyfriend who followed the evolution of this process from the beginning and made me believe that it was possible, a big thank you.

Institutionally I must also thank University Institute of Health Sciences (IUCS, CESPU) which allowed me to do this master degree and dissertation, and to the IINFACTS that provided me with all the necessary equipment and conditions. And also to all the teachers, researchers and technicians involved. To the Centro Hospitalar do Tâmega e Sousa EPE, Penafiel/Portugal, for having provided all the necessary data and biological samples



The results presented in this dissertation are part of the following scientific communication:

#### **Poster communication**

A. Sousa, B. Peixoto, P. Pimenta A. Andrade, V. Gonçalves, S. Leal, C. Ribeiro, DESENVOLVIMENTO DE UM MÉTODO POR CROMATOGRAFIA LÍQUIDA ACOPLADA A DETEÇÃO UV/ FLUORESCÊNCIA PARA A QUANTIFICAÇÃO DE METABOLITOS DA VIA QUINURENINÉRGICA EM PACIENTES COM INSUFICIÊNCIA CARDÍACA, 3ª Reunião Internacional da RACS, Braga, Portugal, 28 and 19 September 2020 (Abstract and poster communication in annex 2).

## RESUMO

O triptofano (TRP) tem um papel importante na síntese de proteínas e de várias substâncias biologicamente ativas. É metabolizado pela via da quinurenina, produzindo uma série de metabolitos ativos tais como o ácido quinurénico (KA), L-quinurenina (KYN), entre outros. Os metabolitos do TRP estão relacionados com processos biológicos como a inflamação, a excitabilidade neuronal, o crescimento celular, o *stress* oxidativo e a divisão celular. Além disso, existem evidências recentes que indicam que os metabolitos do TRP desempenham um papel relevante na fisiopatologia das doenças cardiovasculares através de mecanismos inflamatórios e de stress oxidativo.

A quantificação do TRP e dos seus metabolitos em amostras biológicas pode ser uma poderosa ferramenta para compreender os mecanismos da doença. Assim sendo, é de suma importância desenvolver métodos analíticos capazes de quantificar o TRP e seus metabolitos para que juntamente com parâmetros bioquímicos e marcadores inflamatórios seja possível monitorizar a progressão da doença, sendo também útil em medicina forense.

Assim sendo, o objetivo deste trabalho foi o desenvolvimento e a validação de um método analítico de cromatografia líquida com detetor UV-Vis e fluorescência (FD) (LC-UV-Vis/FD) para análise do TRP, KYN e KA em amostras de urina de doentes com insuficiência cardíaca (IC). Além disso, foram quantificados parâmetros bioquímicos e marcadores inflamatórios utilizando um analisador automático Prestige 24i e um ensaio de imunoabsorção enzimática (ELISA) que foi utilizado para a determinação dos níveis plasmáticos do peptídeo natriurético do cérebro (BNP) correlacionando os dados com os valores do TRP e dos seus metabolitos.

As condições otimizadas do método LC-UV-Vis/FD foram conseguidas utilizando uma coluna analítica, Luna® 3 µm PFP, uma fase móvel constituída por 20 mM de formato de amónia em água ultra pura (com 0,01 % de ácido fórmico), acetonitrilo e etanol (95/2/3, v/v/v), um fluxo de 0,7 mL/min e uma temperatura de 25°C no forno de coluna. Foi utilizado um programa de comprimento de onda ( $\lambda$ ) para o detetor de UV fixado a 365 nm para a KYN e para a 3-nitrotirosina utilizada como

padrão interno, e 344 nm para o KA. Para o detetor FD foi utilizado  $\lambda$  de excitação e emissão de 280 nm e 365 nm, respetivamente para o TRP.

O método foi validado de acordo com as normas da *European Medicines Agency* (EMA) em termos de seletividade, linearidade, limite de deteção (LD), limite de quantificação (LQ), precisão, exatidão e recuperação. Os coeficientes de correlação ( $R^2$ ) foram superiores a 0,99 para todos os compostos. Os LD variaram entre 13,1 ng/mL para KYN e 21,6 ng/mL para TRP e KA. Os LQs foram de 39,8, 65,4 e 83,5 ng/mL para KYN, TRP e KA, respetivamente. O método demonstrou ser exato (82 a 116%) e preciso (abaixo de 15%) e as recuperações variaram entre 95 e 130%.

O método foi aplicado para a quantificação do TRP e dos seus metabolitos em voluntários saudáveis e pacientes homens com IC. Os pacientes foram divididos em dois grupos, diabéticos (DM2/HF) e não diabéticos (HF). A concentração do TRP e dos seus metabolitos foram comparadas entre grupos. Os resultados mostraram que o grupo DM2/HF apresentou valores medianos de KYN mais elevados e KA mais baixos do que os voluntários saudáveis. Pelo contrário, foram encontrados valores medianos mais baixos destes metabolitos no grupo HF do que os dos pacientes DM2/HF e voluntários. As razões KYN/TRP e KA/KYN também foram determinadas. Os resultados apoiam a hipótese de que a razão KYN/TRP está relacionada com a atividade enzimática e que a razão KA/KYN pode ser um bom indicador neuroprotetor. Apesar dos dados do presente estudo terem sido obtidos a partir de um pequeno grupo de pacientes (estudo piloto), os resultados mostraram uma relação entre parâmetros bioquímicos, marcadores inflamatórios e alterações na concentração de TRP, KYN e KA e o potencial do método LC-UV-Vis/FD para a monitorização dos compostos selecionados em pacientes cardíacos.

**Palavras-chave:** triptofano; quinurenina; ácido quinurénico; cromatografia líquida; biomarcadores inflamatórios; doença cardíaca.



## ABSTRACT

Tryptophan (TRP) plays an important role in the synthesis of proteins and various biologically active substances. It is metabolized through the kynurenine pathway, producing a range of active metabolites such as kynurenic acid (KA), L-kynurenine (KYN), among others. TRP metabolites are closely related to processes such as inflammation, neuronal excitability, cell growth, oxidative stress and cell division. In addition, recent evidence indicates the relevant role of the TRP metabolites in the pathophysiology of cardiovascular diseases via inflammatory and stress oxidative mechanisms.

Quantification of TRP and its metabolites in biological samples can be a powerful tool to elucidate the disease mechanisms. Therefore, it is of the utmost importance to develop analytical methods able to quantify TRP and its metabolites in biological matrices that together with biochemical parameters and inflammatory markers may allow monitor the progression of disease, being also useful in forensic medicine. Therefore, the aim of this work was to develop and validate a liquid chromatography with UV and fluorescence detector (FD) (LC-UV-Vis/FD) analytical method for analysis of TRP and its metabolites (KYN, KA) in urine samples from heart failure (HF) patients. Further, biochemical parameters and inflammatory markers were quantified using a Prestige 24i automated analyzer and an enzyme-linked immunosorbent assay (ELISA) was used to determine plasma brain natriuretic peptide (BNP) levels and data correlated with TRP and its metabolite values.

The LC-UV-Vis/FD optimized conditions were achieved using a Luna® 3  $\mu$ m PFP analytical column, a mobile phase consisting in 20 mM of ammonium formate in ultra-pure water (with 0.01 % of formic acid), acetonitrile and ethanol (95/2/3, v/v/v), a flow rate of 0.7 mL/min and column oven set at 25°C. A wavelength ( $\lambda$ ) program was used for the UV detector set at 365 nm for KYN and 3-nitrotyrosine used as internal standard, and 344 nm for KA, while the FD was set to excitation and emission  $\lambda$  of 280 nm and 365 nm, respectively for TRP.

The method was validated according to the European Medicines Agency (EMA) guidelines in terms of selectivity, linearity, limit of detection (LOD), limit of

quantification (LOQ), precision, accuracy, and recovery. The correlation coefficients ( $R^2$ ) were above 0.99 for all compounds. LODs ranged from 13.1 ng/mL for KYN and 21.6 ng/mL for TRP and KA. The LOQs were 39.8, 65.4 and 83.5 ng/mL for KYN, TRP and KA, respectively. The method demonstrated to be accurate (82 to 116%), precise (below 15%) and recoveries varied from 95 and 130%.

The method was applied to the quantification of TRP and its metabolites in healthy volunteers and male HF patients. Patients were stratified by diabetic (DM2/HF) and non-diabetic (HF) groups. Urinary values of TRP and its metabolites were compared between groups. Results showed that DM2/HF group presented higher KYN and lower KA median values than healthy volunteers. Instead, lower median values of these metabolites were found in HF group than those of the DM2/HF patients and volunteers. The KYN/TRP and KA/KYN ratios were also calculated. Results support the hypothesis that KYN/TRP ratio is related with enzymatic activity and that KA/KYN ratio can be a good neuroprotector indicator. Thought data from this study were obtained from a small group of patients (pilot study) results showed a relationship between biochemical parameters, inflammatory markers and changes in the concentration of TRP, KYN and KA and the potential of the LC-UV-FD method for the monitoring of the selected compounds in cardiac patients.

**Keywords:** tryptophan; kynurenine; kynurenic acid; liquid chromatography; inflammatory biomarkers; heart disease.

# INDEX

1. INTRODUCTION .....	1
1.1. Heart failure – from clinical characteristics to the pathophysiology .....	2
1.2. Cardiac dysfunction and tryptophan metabolism .....	5
1.3. Methods for quantification of TRP and its metabolites .....	9
2. AIMS .....	14
3. MATERIALS AND METHODS .....	15
3.1. Chemicals and equipment's .....	15
3.2. Participants .....	16
3.3. Blood and urine sampling .....	17
3.3.1 Control group .....	17
3.4. Biochemical analysis .....	18
3.5. Sample preparation for LC analysis .....	18
3.5.1 Urine samples .....	19
3.6. Optimization of the chromatographic conditions .....	19
3.7. Method validation .....	21
3.8. Statistical analysis .....	24
4. RESULTS AND DISCUSSION .....	25
4.1. Patients characteristics .....	25
4.2. Biochemical parameters .....	29
4.3. Optimization of urine sample preparation procedure .....	34
4.4. Optimization of the chromatographic conditions .....	35
4.5. Method application .....	45
4.5.1 Urine samples from healthy individuals .....	45
4.5.2 Urine samples from HF patients .....	46

4.6 Relationship between biochemical parameters, TRP and its metabolites.....	48
6. CONCLUSION .....	52
6.1 Limitations.....	53
6.2 Future perspectives.....	53
7. BIBLIOGRAPHY .....	54
8. ANNEXES .....	67

## FIGURE INDEX

- Figure 1.** Scheme that shows the relationship between inflammation, oxidative stress and TRP metabolism. \_\_\_\_\_ 6
- Figure 2.** Chromatogram showing the non-reproducibility of the RT using the UV-VIS detector with the mobile phase of 0.01% TFA : ACN (88:12, v/v) at concentration of 500 ng/mL. \_\_\_\_\_ 36
- Figure 3.** Chromatogram showing the non-reproducibility of the RT using the FD detector with the mobile phase of 0.01% TFA : ACN (88:12, v/v) at concentration of 500 ng/mL. \_\_\_\_\_ 36
- Figure 4.** Chromatogram of a mixture of the compounds at 500ng/mL using a mobile phase of 20 mM ammonium formate in UPW with 0.01% formic acid : ACN (87:13, v/v) at pH 4.4 showing the compounds overlap. \_\_\_\_\_ 37
- Figure 5.** Chromatogram of a mixture of the compounds at 500ng/mL using a mobile phase of 20mM ammonium formate in ultra-pure water with 0.01% formic acid : EtOH (91:9, v/v) at pH 4.4 showing the enlargement of the peaks of 3-NT, TRP and KA. \_\_\_\_ 38
- Figure 6.** Chromatogram of a mixture of the compounds at 1 µg/mL using a mobile phase of 20 mM ammonium formate with 0.01% formic acid : ACN: EtOH (95:2:3, v/v/v) at a flow rate of 0.800 mL/min at λ 250 nm UV-VIS detector and at λ<sub>exc/em</sub>= 280/365 nm for the FD detector \_\_\_\_\_ 39
- Figure 7.** Chromatogram of urine spiked with standard of 10 µg/mL overlapping a chromatogram of a mixture of the compounds at 1 µg/mL. \_\_\_\_\_ 39
- Figure 8.** Chromatogram of 5x diluted patient urine sample overlapping a standard of 1 µg/mL with a , UV-VIS detector set at 0 to 17 min at 344 nm and from 17 to 40 min at 365 nm. \_\_\_\_\_ 40
- Figure 9.** Chromatogram of 5x diluted patient urine sample overlapping a standard of 1 µg/mL m with a FD detector set at 280 nm and 365nm for excitation and emission \_ 40

**Figure 10.** Chromatogram of 5 x diluted urine sample from a healthy volunteer with overlapped with 1 µg/mL standard mixture \_\_\_\_\_ 42

## TABLE INDEX

<b>Table 1.</b> Chromatographic methods reported for the quantification of TRP in biological samples. _____	11
<b>Table 2.</b> Experimental conditions tested for the optimization of the separation of TRP, KYN, 3-NT and KA. _____	20
<b>Table 3.</b> Range of nominal concentrations ( $\mu\text{g}/\text{mL}$ ) of the standards used for the calibration curve _____	22
<b>Table 4.</b> Quality control nominal concentrations _____	23
<b>Table 5.</b> Characteristics from all patients _____	27
<b>Table 6.</b> Male patient characteristics _____	28
<b>Table 7.</b> Biochemical data of male patients _____	31
<b>Table 8.</b> Linearity parameters, LOQ and LOD for KYN, KA and TRP _____	43
<b>Table 9.</b> Accuracy, Intra-day and inter-day precision. _____	44
<b>Table 10.</b> Recovery _____	44
<b>Table 11.</b> Quantification of TRP, KYN and KA in the urine sample of healthy individuals	46
<b>Table 12.</b> Quantification of TRP and its metabolites in the urine sample of male patients in DM2/HF and HF groups and KYN/TRP and KA/KYN ratios. _____	47

## LIST OF ABBREVIATIONS, SYMBOLS AND ACRONYMS

3-HKYN – 3-hidroxykynurenine

3-NT - 3-nitro-tyrosine

AANS - American Association of Neurological Surgeons

ACN - Acetonitrile

ALP - Alkaline phosphatase

ALT - Alanine aminotransferase

ASNR - American Society of Neuroradiology

AST - Aspartate aminotransferase

BMI – Body mass index

BNP – Brain natriuretic peptide

CIRA - Canadian Interventional Radiology Association

CIRSF - Cardiovascular and Interventional Radiology Society of Europe

CK - Creatine kinase

CNS - Congress of Neurological Surgeons

CVD - Cardiovascular diseases

DBP - Diastolic blood pressure

DF - Dilution factor

DM2 - Diabetes mellitus type 2

EF - Ejection fraction

eGFR – Estimated glomerular filtration rate



EIA - Enzyme-linked immunosorbent assay

EMA – European Medicines Agency

ENRS - European Society of Neuroradiology

ESMINT - European Society of Minimally Invasive Neurological Therapy

ESO - European Stroke Organization

EtOH - Ethanol

GC-MS - Gas chromatography coupled to mass spectrometry

HDL-c –High density lipoprotein cholesterol

HF – Heart failure

HFrEF - HF with reduced EF

HPLC-DAD - High performance liquid chromatography coupled to diode array detector

IDO – Indolamine 2.3 - dioxygenase

IFN- $\gamma$  – Interferon gamma

IL-17 - Interleukin 17

IL-1 $\beta$  - Interleukin 1 beta

IL-6 - Interleukin 6

IS – Internal standard

KA – Kynurenic acid

KAT – Kynurenine aminotransferase

KMO – Kynurenine monooxygenase

KYN - Kynurenine

LC-MS/MS - Liquid chromatography tandem mass spectrometry

LDH - Dehydrated lactate

LDL-c – Low density lipoprotein cholesterol

LOD - Limit of detection

LOQ - Limit of quantification

MeOH – Methanol

M.P. – Mobile phase

NAD - Nicotinamide adenine dinucleotide

NK cell – Natural killer cell

NT-proBNP - N-terminal pro-B-type natriuretic peptide

P – Plasma

PP – Protein precipitation

QA – Quinolinic acid

QC – Quality control

r.p.m - Rotations per minute

ROS – Reactive oxygen species

RSD - Relative standard deviation

RT – Retention time

S - Serum

SBP – Systolic blood pressure

SCAI - Society for Cardiovascular Angiography and Interventions

SD – Standard deviation

SIR - Society of Interventional Radiology

SNIS - Society of NeuroInterventional Surgery

SPSS - Statistical Package for the Social Sciences

TDO – Tryptophan 2.3 - dioxygenase

TFA - Trifluoroacetic acid

TNF- $\alpha$  – Tumor necrosis factor alfa

TRP – Tryptophan

U - Urine

UPW – Ultra pure water

WHO - World Health Organization

WSO - World Stroke Organization

XA – Xanthurenic acid

## 1. INTRODUCTION

Non-communicable diseases remain the leading cause of death worldwide and cardiovascular diseases (CVD) account for the major part of premature death followed by cancer, chronic pulmonary disease and diabetes (Mathers *et al.* 2017; WHO 2017; Hasanzad *et al.* 2019; Timmis *et al.* 2020). Most of the cardiovascular deaths results from ischaemic heart disease (myocardial infarction) and ischaemic stroke (cerebral infarction), which are the leading causes of mortality under 75 years in Europe (de la Torre 2004; Nichols *et al.* 2014; Mathers *et al.* 2017; Wilkins *et al.* 2017; Hasanzad *et al.* 2019; Timmis *et al.* 2020). In addition, cardiovascular conditions impose a huge burden in morbidity and disability particularly for elderly people (Benjamin *et al.* 2017). CVD includes all diseases of the heart and circulation system such as coronary heart disease, cardiomyopathies, cerebrovascular disease, peripheral arterial disease among other conditions (Hasanzad *et al.* 2019). Furthermore, clinical events caused by CVD have been associated with an increased risk of vascular dementia and Alzheimer's disease (de la Torre 2004; Mathers *et al.* 2017; Doehner *et al.* 2018). Hypertension, dyslipidaemia, diabetes and obesity are defined as the main risk factors for developing CVD, as well as health risk behaviours such as smoking, alcohol, unhealthy diet and physical inactivity (Mathers *et al.* 2017; WHO 2017; Timmis *et al.* 2020). Moreover, neurological and physiological disorders have been associated with CVD, which can contribute to a worse CVD prognosis (de la Torre, 2004; Rutledge *et al.* 2006; Nikkheslat *et al.* 2015; Heidi *et al.* 2017; May *et al.* 2017; Doehner *et al.* 2018). For example, depression is common among CVD patients with type 2 diabetes mellitus and was associated with more adverse health effects (Thevandavakkam *et al.* 2010). Despite the uncertainty of whether treating major depression reduces the associated risk for CVD mortality, it might be fruitful to consider whether poor outcomes of cardiac patients can be mitigated. To do this, firstly, is needed to identify biomarkers or accurate methods useful for screening, giving support to diagnosis and prognosis. Therefore, it is

crucial to better understand the pathophysiology of CVD and search pathways that can help to orientate the therapeutic approaches in cardiac patient.

## **1.1. Heart failure – from clinical characteristics to the pathophysiology**

Heart failure (HF) is a progressive disease, with frequent hospitalization, reduced quality of life and high mortality (Mosterd and Hoes 2007; Braunwald 2008; Ziaei and Fonarow 2016). Its prevalence is higher among the elderly and represents the leading cause of death (Ziaei and Fonarow 2016). HF is caused by a wide range of abnormalities of myocardial structure or function, characterized by the impairment of ventricular filling or ejection of blood or both (Hunt *et al.* 2001). Whether HF is caused by primary damage to the myocardial muscle or secondary to chronic excessive workload leading to a defective cardiac contraction (Hunt *et al.* 2001). Many conditions can lead to this clinical syndrome such as coronary artery disease, hypertension, cardiomyopathies, congenital heart diseases and arrhythmias, but also the exposition to cardiotoxic substances (e.g. alcohol) (Mosterd and Hoes 2007; Piano and Phillips 2014). Moreover, modifiable risk factors such as impaired glucose tolerance, unfavorable lipid profile, obesity, sedentary lifestyle and cigarette smoking can predispose the development of HF (Mosterd and Hoes 2007).

HF is categorized as systolic and/or diastolic (Hunt *et al.* 2001) and according to the percentage of the ejection fraction (EF), being stratified as reduced (less than 40%), preserved (more than 50%) or mildly reduced EF (Vedin *et al.* 2017). In the HF diagnosis, an increase in natriuretic peptide concentrations, namely brain natriuretic peptide (BNP) and/or N-terminal pro-B-type natriuretic peptide (NT-proBNP) are considered a hallmark, being an independent predictor of cardiovascular events and overall mortality (Rocca and Wijk 2019). More recently, it has shown that BNP and NT-proBNP can also be useful in forensic medicine as postmortem biomarkers of cardiac dysfunction (Cao *et al.* 2019). HF with reduced EF, it is characterized by systolic dysfunction and reduced cardiac output causing negative consequences on end-organ perfusion (e.g. brain and kidney), activation of neurohormonal (e.g. renin-angiotensin-aldosterone system, sympathetic nervous system) and

inflammatory systems, contributing to the worsening of cardiac function (NHFA CSANZ Heart Failure Guidelines Working Group *et al.* 2018). The inability of the left ventricle to relax or contract properly can occur due to cardiomyocyte hypertrophy, cardiomyocyte loss, fibrosis and/or inflammation (Vedin *et al.* 2017; Boer *et al.* 2018).

Inflammation is a response of the organism to restore tissue homeostasis after injury or infection (Linthout and Tschöpe 2017). The inflammatory process can be triggered by heart disease (Linthout and Tschöpe 2017; Shirazi *et al.* 2017) as well as by other pathologies such as obesity (de Mello *et al.* 2018) and diabetes (Rehman and Akash 2017). Nevertheless, this biological mechanism is implicated in the pathogenesis and progression of HF including HF-underlying comorbidities such as diabetes and obesity (Linthout and Tschöpe 2017). Regarding heart disease, inflammation can act as a compensatory response to injury to protect cardiac morphology and function, but in a chronic inflammatory state it has detrimental effects for the heart (Shirazi *et al.* 2017). The inflammatory process involves the activation of innate immune system (e.g. monocytes, NK cells and dendritic cells) and adaptive immune system (B cells and T cells) (Ayoub *et al.* 2017). Consequently, to the activation of immune cells, there is an increase of pro-inflammatory cytokines and growth factors, namely interleukin-1 $\beta$  (IL-1 $\beta$ ), interleukin-6 (IL-6), interleukin-17 (IL-17), interleukin-18 (IL-18), tumor necrosis factor- $\alpha$  (TNF- $\alpha$ ) and interferon- $\gamma$  (IFN- $\gamma$ ) (Shirazi *et al.* 2017), which have been implicated in the pathogenesis of HF (Linthout and Tschöpe 2017; Shirazi *et al.* 2017). These signaling molecules can induce cardiomyocyte hypertrophy and apoptosis, fibrosis, and ultimately lead to adverse cardiac remodeling (Shirazi *et al.* 2017). In addition, inflammatory pathways interplay with neurohormonal activation and oxidative stress, which includes the formation of angiotensin II and reactive oxygen species (ROS) (Ayoub *et al.* 2017).

Excessive ROS levels are responsible for an impairment of the redox balance inducing oxidative stress, which leads to cell damage that can culminate in cell death (Dröge 2002; Valko *et al.* 2007). An increased ROS formation can be caused by endogenous (e.g. inflammation, elevation in O<sub>2</sub> concentration, and increased mitochondrial leakage) and/or exogenous conditions (e.g. smoking, nutrition,

psychological and emotional stress) (Valko *et al.* 2007). High levels of ROS causes DNA damage, protein and lipid modification, lipid peroxidation, inhibition of mitochondrial enzymes and, can also trigger cell death pathways (Li and Trush 2016). ROS molecules are produced by cardiomyocytes and endothelial cells of blood vessels of the heart (Li *et al.* 2020). Under physiological conditions, ROS play a key role in the heart, being linked to the regulation of development and maturation of cardiomyocytes (Karam *et al.* 2017) with action in cardiac excitation–contraction coupling and in the control vascular tone (Kattoor *et al.* 2017). Under pathological conditions, the higher production of ROS is associated with a decrease in anti-inflammatory enzymes and peroxisomal catalysis, alters the cardiac contractibility through the modification of the opening of the ionic channels and the phosphorylation of troponin T by kinases and high density lipoprotein (Peoples *et al.* 2019). Moreover, the activation of ROS pathways is implicated in the cardiomyocytes hypertrophy, fibroblasts proliferation and apoptosis, which are cellular processes that contribute to cardiac remodeling (Hu *et al.* 2016). Lipid peroxidation is another consequence of oxidative stress induced by ROS and has been associated with alteration of the dynamic of membrane structure, including dysfunction and permeability (Niki 2008). In addition, the oxidative pathway is also involved in the oxidation of low density lipoprotein cholesterol (LDL-c) to pro-atherogenic forms (Fetoni *et al.* 2019), which is an important factor in the development of arteriosclerosis (Niki 2008). Moreover, oxidation of LDL-c is considered as a pro-inflammatory and immunogenic factor that can contribute to chronic inflammation (Rhoads and Major 2018).

Oxidative stress also leads to a failure in energy biosynthesis with implications in several cardiac pathological conditions such as alcoholic cardiomyopathy, diabetic cardiomyopathy and HF, as well as in other chronic disease such as diabetes and obesity (Li *et al.* 2020). However, obesity has a proper mechanism to generate oxidative stress, the process seems to be initiated by mitochondrial dysfunction that can trigger the stimulation of pro-inflammatory cytokines production (Koliaki *et al.* 2019). Therefore, the decrease in the oxidative capacity of the cell leads to a decrease in oxygen consumption and, consequently, there is a decrease in energy biosynthesis causing metabolic deregulation and an increase of ROS formation in fat

tissue, which are processes that contribute to vascular dysfunction and chronic inflammation (Kattoor *et al.* 2017). In addition to the ROS signaling molecules, the release of pro-apoptotic cytochrome-c triggers programmed cell death (Arimon *et al.* 2015). Mitochondrial oxidative stress seems to have a crucial role in the transition from hypertrophy to heart failure (Peoples *et al.* 2019). However, mitochondrial dysfunction in HF is not only responsible for higher ROS formation but also for an impairment of bioenergetic supply/demand of cardiomyocytes, interfering in the processes of contraction and relaxation (Peoples *et al.* 2019).

## **1.2. Cardiac dysfunction and tryptophan metabolism**

To address the great need of advancing CVD management, several mechanisms implicated in the pathophysiology of HF have been investigated as potential targets, namely inflammation, oxidative stress and others. Among putative candidates, tryptophan (TRP) metabolites received attention with a recently renewed interest on the inflammatory perspective (Sorgdrager *et al.* 2019). TRP is an essential aromatic amino acid that must be supplied by the diet, although only small amounts are necessary in human healthy nutrition (Heine *et al.* 1995). Apart from its role as one of the rate-limiting amino acids in protein synthesis (Marcos *et al.* 2016) it is the only source of substrate for the production of several bioactive molecules implicated in the modulation of central nervous and immune systems (Rutledge *et al.* 2006; Wang *et al.* 2015). Furthermore, TRP is the precursor for the synthesis of important neurotransmitters such as serotonin and tryptamine, as well as for the synthesis of nicotinic acid and melatonin (Heine *et al.* 1995). It plays an essential role in the homeostasis of the body, partly due to its antioxidant effect and lipid peroxidation inhibitor role (Zou 2015). The majority of free TRP undergoes oxidative metabolism through the kynurenine pathway, which generates multiple TRP metabolites, collectively known as kynurenines (Marcos *et al.* 2016) and the enzyme cofactor nicotinamide adenine dinucleotide (NAD) that participates in many cellular processes (Sadok *et al.* 2017). There is growing evidence that TRP metabolism may exert profound effects by activating or inhibiting metabolism and immune



responses (Wirleitner *et al.* 2003). A deregulation between TRP input and its catabolism can trigger the pathway to generate oxidative stress (figure 1), increase the overall inflammatory state (Marcos *et al.* 2016) and activate the immune system (Zou 2015).

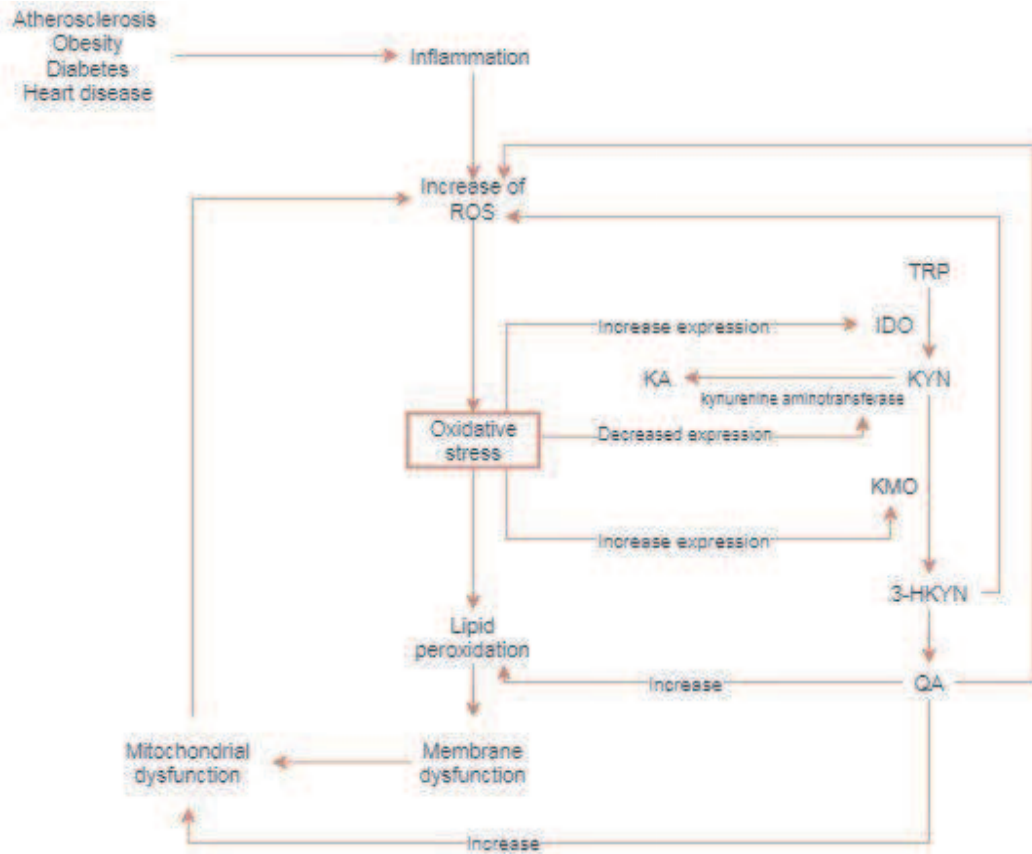


**Figure 1. Scheme that shows the relationship between inflammation, oxidative stress and TRP metabolism.** [3-hydroxykynurenine (3-HKYN); indoleamine 2,3-dioxygenase (IDO); kynurenic acid (KA); kynurenine (KYN); kynurenine monooxygenase (KMO); quinolinic acid (QA); tryptophan 2,3-dioxygenase (TDO); tryptophan (TRP)].

The kynurenine pathway can be divided into two parts, depending on the enzyme that step in TRP metabolism. Normally, TRP is metabolized by tryptophan 2,3-dioxygenase (TDO) located in the liver (Thackray *et al.* 2008), being crucial for the regulation of the amino acid concentration in plasma (Sadok *et al.* 2017). On the other hand, the metabolism of TRP can also be performed by indoleamine 2,3-dioxygenase (IDO) which is present in extrahepatic tissues such as central nervous system, endocrine system, lung and epithelial tissue (Zou 2015). This wide location

serves for IDO to exhaust the TRP in different localizations, depriving them of this amino acid and causing an accumulation of metabolites that can somehow be toxic (Zou 2015). Thus, under normal conditions, the degradation is performed by TDO, whereas in inflammation states, is the IDO that begins the TRP catabolism (Badawy 2017). Although the two enzymes are activated under different circumstances, the degradation product is the same, *N*-formylkynurenine. This intermediate metabolite is unstable and serves as a substrate for the action of formidase (Pertovaara *et al.* 2007), resulting in the formation of kynurenine (KYN) (Liu *et al.* 2019). KYN is a stable metabolite and it can have harmful effects, through its contribution in the formation of ROS and in cell death (Zou 2015).

KYN can continue in kynurenine pathway, being a substrate for three different enzymes: kynurenine monooxygenase (KMO) (Connor *et al.* 2008), kynureninase and kynurenine aminotransferase (KAT) (Esquivel *et al.* 2017), all producing different metabolites (Polyzos and Ketelhuth 2015). KMO is found predominantly in the microglia (Thevandavakkam *et al.* 2010) and is activated by inflammatory processes (Connor *et al.* 2008), resulting in the formation of 3-hydroxykynurenine (3-HKYN), considered to have prooxidant effects in the apoptotic and cytotoxic processes (Cervenka *et al.* 2017). Kynureninase is expressed at higher levels under inflammation (Sadok *et al.* 2017) and is responsible for the formation of 3-hydroxyanthranilic acid, which is rapidly converted into quinolinic acid (QA) (Liu *et al.* 2019), a metabolite closely linked to mitochondrial dysfunction, lipid peroxidation (Zou 2015), apoptosis and cytotoxicity (Song *et al.* 2017). Finally, in physiological conditions, there is an increase of the expression of KAT with the formation of kynurenic acid (KA), which has beneficial effects due to its anti-inflammatory properties and preventive action in the lipid peroxidation and in the formation of ROS (Zou 2015). Furthermore, KAT can also metabolize 3-hydroxyanthranilic acid with the formations of xanthurenic acid (XA) (Gobaille *et al.* 2008). Despite some similarity in the structure of XA and KA, each metabolite formed by the action of KAT has different effects (Sadok *et al.* 2017), namely XA is involved in the control of the 3-hydroxyanthranilic acid plasma concentration (Stone 2001) and therefore, opposing the QA effects in lipid peroxidation (Zou 2015), apoptotic and cytotoxic processes (Thevandavakkam *et al.* 2010).

The kynurenine pathway plays a critical role in the balance of the redox state (Karu *et al.* 2016), since the degradation of TRP can produce several bioactive metabolites, which can be antioxidant and prooxidant (Moffett and Namboodiri 2003). The redox state is dynamic, being highly influenced by inflammation, oxidative stress and lipid peroxidation, which provide a milieu suitable for the kynurenine pathway catabolism (Zou 2015) and the redox capacity of its metabolites can influence biological functions that are controlled by redox-responsive signaling pathways (Esquivel *et al.* 2017). Nevertheless, dysregulation of the kynurenine pathway has been linked to various diseases, including CVD, neurodegenerative disorders, depression, diabetes and cancer (Zuo *et al.* 2016; Lehrke and Marx 2017; Song *et al.* 2017; Wigner *et al.* 2018). Moreover, it has been shown that TRP metabolites such as KYN, 3-HKYN and XA can predict the increased risk of poor outcomes of patients with CVD (Zuo *et al.* 2016). Alongside to the role of kynurenine pathway in regulating immune system functions, redox state and inflammation, emerging evidence indicates that TRP metabolites can be involved in cardiovascular pathology (Song *et al.* 2017). However, it is still unclear whether endogenous kynurenines directly contribute to the initiation or promotion of CVD development. Therefore, it is important to further study and improve our understanding of the effects of TRP metabolites on initiation and progression of CVD. In order to elucidate its role on disease mechanisms, the monitoring of kynurenines metabolites it is an essential step. Thus, finding an accurate method with higher reproducibility can contribute to that goal. Moreover, TRP metabolites have potential as a marker to evaluate the outcomes of therapeutic choices, which is an attractive tool that can be applied to prevent the poor outcomes of CVD.

### 1.3. Methods for quantification of TRP and its metabolites

Some methods have been reported for the analysis of TRP and its metabolites in biological samples mostly based on liquid (LC) and gas (GC) chromatography (Table 1). Nonetheless, LC methods with various detection modalities such as ultraviolet detection (UV), diode array (DAD), fluorescence detection (FD) or mass spectrometry (MS) are the most used. Different samples have been used for the analysis of TRP and its metabolites such as plasma, serum and urine though plasma is among the most used and for different purposes. Nevertheless, due to the complexity of the biological matrices and the low concentrations of the analytes present, sample preparation procedures are required prior to the chromatographic analysis in order to reduce matrix interferences and for the pre-concentration of target compounds. The reported sample preparation procedures were centrifugation for urine samples while for plasma and serum protein precipitation (Table 1).

Considering LC methods, selection of the coupling detector depends on the availability and requirements concerning sensitivity, selectivity, matrix, and cost. Even though, a trend is seen towards the used of LC-MS and LC tandem mass spectrometry (LC-MS/MS) methods due to their greater sensitivity, i.e., lower limit of quantification (LOQ) in the order of nanograms/mL (Zhu *et al.* 2011) and information on the chemical structural of target compounds (Oh *et al.* 2017; Want, 2018). Nevertheless, some limitations such as matrix effect, expensive equipment costs, complex optimization of tandem mass parameters are some of LC-MS drawbacks.

Tong *et al.* (2018) reported a LC-MS/MS for the simultaneous determination of TRP and its metabolites including KYN, KA, XA and 5-hydroxytryptamine (5-HT) in human plasma. Chromatographic separation was achieved using a C18 column in a total run time of 3.5 min. The method was applied to the quantification of the compounds in plasma samples from healthy volunteers and myocardial infarction patients. A LC-MS/MS method for analysis of TRP and nine metabolites (including KYN and KA) in human plasma were also reported (Chen *et al.* 2019). Chromatographic conditions were obtained using a Waters Acquity UPLC HSS T3 reversed-phase column (3.0 mm × 100 mm, 1.8 μm) with a mobile phase consisting

in 0.1% formic acid in water and acetonitrile in a gradient elution mode. The method was applied to study the clinical characterization of TRP metabolism in healthy volunteers. A LC-MS/MS method was also established for determining TRP, KYN and KA in human serum. Separation was achieved on an Agilent Eclipse XDB-C18 (4.6 mm × 150 mm, 5 μm). Two conditions were optimized, one with methanol/water (45:55, v/v) containing ammonium formate (5 mM) for analysis of TRP and KYN and other with methanol/water (35:65, v/v) containing ammonium formate (5 mM) for KA. The method was applied to healthy volunteers and depression patients. A LC method for the quantification of TRP and KYN in rat serum samples were reported using a FD (Zagajewski *et al.* 2012). In that method, the simultaneous determination of TRP, six metabolites and melatonin were possible using UV and a fluorometric detector with multiple wavelengths. Separation was performed using a nucleosil Supelco C18 5 μm 4.6 mm × 250 nm column with a mobile phase consisting in water/0.1% trifluoroacetic acid (TFA) and methanol/0.1% TFA in gradient elution. The method showed to be selective, sensitive and was applied to the study of kinetics and TRP metabolism in gastrointestinal tract. Vignau *et al.* (2004) also reported a LC using FD able for the quantification of TRP and KYN in serum samples. Urine samples were also used for the analysis of TRP and its metabolites. This biological sample it is easier to collect and is less invasive and thus can be an alternative to other biological samples. For instance, a LC-MS method was developed and validated for study the urinary profile of TRP, KYN, serotonin, and tryptamine in patients with metabolic syndrome (Oh *et al.* 2017). Sun *et al.* (2019) also proposed a fast chemometrics-assisted HPLC-DAD method for quantification of eight small molecules including TRP. This method showed satisfactory resolution and quantification taking into account the complex matrix interferences from the urine samples.

GC methods has also been reported though less used probably due to the necessity of derivatization to allow volatility of the compounds (Shin *et al.* 2017).

Table 1. Chromatographic methods reported for the quantification of TRP in biological samples.

Analyte	Matrix	Sample preparation procedure	Analytical conditions	Method	LOQ	Reference
TRP, KYN, KA	P	PP with ACN containing 1% formic acid. After being vortexed and centrifuged at 12000 rpm for 10 min, supernatant was evaporated under nitrogen gas flow and reconstituted in water containing 0.1% formic acid.	C18 HPLC column (50 × 2.1 mm, 5 µm) with M.P. (A) water containing 0.1% formic acid and (B) ACN containing 0.1% formic acid at flow rate of 0.5 mL/min	LC/MS	2 µg/mL; 0.2 µg/mL; 0.4 µg/mL	(Tong <i>et al.</i> 2018)
TRP, KYN	Rat S	2-fold dilution in potassium phosphate buffer. followed by PP, vortex and centrifuge for 10 min at 11000 g and finally filter with 0.2 µm filter	Supelco C18 (4.6×250 mm i.d.) with M.P. (A): water with 0.1% TFA and (B) MeOH with 0.1% TFA. at flow of 1.0 ml/min	HPLC-FD	5.9x10 <sup>-7</sup> µg/mL; 2.1x10 <sup>-4</sup> µg/mL	(Zagajewski <i>et al.</i> 2012)
TRP	U	PP and incubate sample at -20 °C for 20 min followed by centrifuged at 12000 r.p.m. for 5 min at 4 °C	T3 column (100 mm × 2.1 mm i.d., 3.0 µm particle size) with M.P. (A) 0.1% formic acid in water and (B) 0.1% formic acid in ACN at a flow rate of 0.2 mL/min	LC-MS/MS	0.05 µg/mL	(Oh <i>et al.</i> 2017b)
TRP, KYA, KA	S	PP with MeOH. The residue was redissolved in MeOH/water	C18 column (4.6 mm × 150 mm, 5 µm) The M.P. for Trp and Kyn was MeOH/water (45:55, v/v) containing ammonium formate (5 mM) and the M.P. for KA was MeOH/water (35:65, v/v) containing ammonium formate (5 mM) at flow rate 0.5 mL/min.	LC/MS/MS	1 µg/mL; 0.1 µg/mL; 0.001 µg/mL	(Hu <i>et al.</i> 2017)
TRP, KYN	S	Serum samples serial dilutions and PP with perchloric acid (8%) followed by centrifugated for 10 min at 64 g	C18 column (150 × 4.6 mm) with M.P. mixture of 5 mmol L <sup>-1</sup> aqueous zinc acetate solution and ACN (92:8; v/v) at flow rate 1.0 mL min <sup>-1</sup>	HPLC FD	0.0016 µg/mL; 0.0006 µg/mL	(Vignau <i>et al.</i> 2004)
TRP	P	PP with perchloric	C18 column (150 x 4.6 mm)	HPLC UV-	0.50 µg	(Pinhati <i>et</i>

		acid (8%) followed by centrifuged for 15 min at 1200g	with M.P. (A) aqueous solution of sodium acetate (AcNa) (5 mM) and M.P. (B) ACN (92:8, v/v) at flow rate 1 mL min <sup>-1</sup>	VIS	/mL	<i>et al.</i> 2012)
KYN, TRP	S	Serum was diluted with phosphate buffer and deproteinised by cooled EtOH followed by centrifugation 14,000g, 10 min and finally supernatant was filtered using 0.2 µm pore size filter.	Columns RP18e (4.6 mm × 50 mm, 3.0 mm × 100 mm) with M.P. 15 mmol/L phosphate buffer (KH <sub>2</sub> PO <sub>4</sub> + K <sub>2</sub> HPO <sub>4</sub> ·3H <sub>2</sub> O) at flow rate 1 mL/min (0–3.09 min) and 2.3 mL/min (3.10–8.20 min)	HPLC – DAD and FD	0.042 µg/mL; 0.102 µg/mL	(Krcmova <i>et al.</i> 2011)
KA, TRP, KYN	P	Extraction with formic acid (1%) followed by dried for 5-10 min per application low vacuum, finally it was reconstituted with 1% NH <sub>4</sub> OH in water: MeOH	C18 column Aqueous column (100 × 2.1 mm) with M.P. (A) ammonium formate in water 0.05% and (B) ACN at flow rate 0.2 mL/min	LC–MS/MS	0.00066 µg/mL; 0.00071 µg/mL; 0.0007 3µg/mL	(Möller <i>et al.</i> 2012)
TRP	U	Derivatization and extraction process	C18 column (100 × 2.1 mm, 1.7 µm) with M.P. (A) 0.1% formic acid in water and (B) MeOH at flow rate 0.2 mL/min	LC-MS	0,0003 µg/mL	(Lee <i>et al.</i> 2017)
TRP	U	Centrifuged at 10000 r.p.m. under 4 °C for 15 min followed by dilutes with ultrapure water	C18 reversed-phase column (150 mm × 4.6 mm i.d.) with M.P. (A) 20 mmol L <sup>-1</sup> ammonium acetate and (B) MeOH at a flow rate of 1.0 mL min <sup>-1</sup>	HPLC-DAD	0.173 µg/mL	(Sun <i>et al.</i> 2019b)
TRP	U	Hydrolysis procedure and SPE cartridge was applied for rapid cleanup. The cartridge was dried applying full vacuum,	DB-5MS capillary column (20 m × 0.25 mm i.d.) Helium was used as the carrier gas at a flow rate of 1.0 mL/min. flow rate of Nitrogen as the collision gas was set to 1.5 mL/min	GC-MS	not described	(Shin <i>et al.</i> 2017)
TRP; KYN; KA	P	The mixture (ACN + IS + P) was vortexed for 4 min, incubated for 10 min at -20 °C for PP and then centrifuged for 20 min at 4 °C.	T3 reversed-phase column (3.0 mm × 100 mm,) with the M.P.(A) (0.1% formic acid in water, v/v) and (B) (100% ACN) at a flow rate of 0.3 mL/min.	LC-MS	0.1 µg/mL; 0.025 µg/mL; 0.005 µg/mL	(Chen <i>et al.</i> 2018)
TRP, KYN,	U	Centrifuged at 12,000	Agilent HC-C18 (2)	L.C-UV/FD	Not	(Zhao <i>et</i>

KA		rpm for 5 min at 4 °C to PP. h supernatant was diluted with distilled water.	analytical column with M.P.(A) (20 mmol/L NaAc, 30 mmol/L HAc and 3% MeOH) and (B) (20 mmol/L NaAc/HAc, 10% MeOH and 10% ACN) at flow rate 1 mL/min.		described	<i>et al.</i> 2011)
----	--	--	--	--	-----------	---------------------

ACN: Acetonitrile; EtOH: Ethanol; GC-MS: Gas chromatography-mass spectrometry; HPLC-DAD: High performance liquid chromatography with a diode-array detector; IS: Internal standard; KA: kynurenic acid; KYN: kynurenine; KH<sub>2</sub>PO<sub>4</sub>: Potassium dihydrogen phosphate; LC-MS/MS: Liquid chromatography tandem mass spectrometry; MeOH: Methanol; M.P.: mobile phase; NH<sub>4</sub>OH: Ammonium hydroxide; P: Plasma; PP: Protein precipitation; S: Serum; TFA: trifluoroacetic acid; TRP: tryptophan; U: Urine.



## 2. AIMS

To develop an analytical method by liquid chromatography coupled to a UV-Vis/fluorescence detector (LC-UV-Vis/FD) used for the quantification of TRP and its metabolites (KYN and KA) in biological samples.

To validate the method according to international guidelines from European Medicines Agency (EMA).

To characterize the cardiac patients of the present study, including the quantification of several biomarkers in serum samples.

To quantify TRP and its metabolites (KYN and KA) in biological specimens from patients with heart failure (HF), elucidating biological and pathological variation.

### 3. MATERIALS AND METHODS

#### 3.1. Chemicals and equipment's

HPLC grade solvents as acetonitrile (ACN, >99.9%), ethanol (EtOH, >99.8%) and methanol (MeOH, >99.9%) were purchased from Fisher Scientific UK (Leicestershire, United Kingdom). Ultra-pure water (UPW) was obtained from a SG Ultra Clear UV plus equipment. Glass microfibers filter with 0.7  $\mu\text{m}$  porous size were purchased from VWR (Leuven, Belgium). Formic acid was obtained from Finland (EMSURE®, Finland); trifluoroacetic acid (TFA) was purchased from Acros Organics (Geel, Belgium). Tryptophan (TRP) both with purity > 99% was obtained from Sigma-Aldrich (Shanghai, China), kynurenine (KYN) and 3-nitro-tyrosine (3-NT) were purchased from Sigma-Aldrich (Buchs, Switzerland), kynurenic acid (KA) from Sigma-Aldrich (Dorset, United Kingdom) and ammonium formate (>99%) was purchased from Sigma-Aldrich (Bangalore, India). Individual standards stock solutions were prepared at 1 mg/mL in MeOH and stored in amber bottles at  $-20^{\circ}\text{C}$ . Working standard solutions were freshly prepared and obtained by dilution of stock solutions in appropriate solvent, i.e., MeOH or 20 mM of ammonium formate in UPW (with 0.01% of formic acid). For biochemical analysis, alkaline phosphatase (ALP), alanine aminotransferase (ALT), aspartate aminotransferase (AST), creatine kinase (CK), dehydrated lactate (LDH), C-reactive protein, total cholesterol, high-density lipoprotein cholesterol (HDL-c), low-density lipoprotein cholesterol (LDL-c), creatinine, urea, uric acid, total bilirubin, triglycerides and glucose were purchased from Cormay (Poland). Sodium ( $\text{Na}^+$ ), magnesium ( $\text{Mg}^{2+}$ ), calcium ( $\text{Ca}^{2+}$ ) and chloride ( $\text{Cl}^-$ ) were obtained from Spinreact (Spain). Human BNP commercial EIA kit was purchased from RayBiotech (Georgia, USA).

Chromatographic analysis was performed using LC equipment Shimadzu UFLC Prominence System coupled to a ultraviolet/ visible (UV/Vis) and fluorescence detector (LC-UV/Vis and LC-FD) and equipped with two pumps LC-20AD, an autosampler SIL-20AC, a column oven CTO-20AC, a degasser DGU-20A5, a system controller CBM-20A and an LC Solution, Version 1.24 SP1 (Shimadzu Corporation,

Tokyo, Japan). The FD coupled to the HPLC system was a Shimadzu RF-10AXL and the UV/Vis was a Shimadzu SPD-20A. The analytical column was a Luna® 3 µm PFP (2) 100<sup>o</sup> (Phenomenex, Portugal). A centrifuge Heraeus Biofuge Pico and a centrifuge Refrigerated Heraeus Biofuge 1.0R were also used.

### 3.2. Participants

A total of 22 patients enrolled in the “Biomarcadores inflamatórios, metabolitos do triptofano e, o risco de disfunção cognitiva em pacientes com insuficiência cardíaca” (Heart&Mind) study were included in this part of the experimental approach to analyse biological specimens from patients. The Heart&Mind is a pilot, observational study of stable patients with HF that aims to evaluate TRP metabolites as a potential biomarker of the link between cognitive dysfunction and cardiac disease. Patients were recruited during their regular cardiology consultation, in the Centro Hospitalar do Tâmega e Sousa, EPE, from September 2017 to December 2018. To be eligible for this study, HF patients had to be diagnosed for more than 6 months ago (i.e. they should not have been hospitalized for HF in the past six months) and evidence of systolic dysfunction ( $EF \leq 40\%$ ). Exclusion criteria included having an actual or previous history of neurological and psychiatric pathology; sensory and motor disabling of neurocognitive evaluation; excessive consumption of alcoholic beverages, alcoholism and narcotics use; occurrence of infection or inflammation in the last month. In the visit, the research physician performed a short medical evaluation, anthropometric parameters (weight, height, and abdominal circumference) were measured urine and blood samples were collected. Additional information about medical history, cardiovascular disease risk factors (e.g. DM type 2 (DM2) and hypertension) and medications were collected from medical records and interview conducted by the nutritionist during the project. Body mass index (BMI) was calculated as body weight (in kilograms) divided by the square of height (in meters) and values expressed as  $kg/m^2$ . BMI cut-off points were used to classify patients according on the World Health Organization (WHO) definition of

underweight (BMI value of  $< 18.5$ ), normal weight (BMI value of  $18.5-24.9$ ), overweight (BMI value of  $25.0-29.9$ ) and obesity (BMI value of  $\geq 30.0$ ).

The study fulfilled the Declaration of Helsinki and was approved by Committee for Medical and Health Research Ethics of the Centro Hospitalar do Tâmega e Sousa, EPE. Written informed consents were obtained from all participants.

### **3.3. Blood and urine sampling**

Blood and spot urine samples of HF patients were collected at the hospital facilities. The blood samples were obtained by arm venipuncture and collected using BD Vacutainer® tubes and anticoagulant-treated tubes. Serum samples were obtained after coagulation of whole blood for 15-30 minutes at room temperature and centrifuged to separate the clot. Plasma samples were obtained from whole blood collected in citrate-treated tubes and centrifuged for at least 12 minutes at room temperature. Serum and plasma supernatant were transferred into 2 mL Eppendorf vials and urine samples were transferred into 15 mL Falcon tubes, using a Pasteur pipette and aliquots were stored at  $-20^{\circ}\text{C}$  until analysis.

Urine specimens of patients excluding one missing sample ( $n = 21$ ) were used for the development of the analytical method, LC-UV-VIS/FD and analyzed for the quantification of TRP and its metabolites. Additional biochemical analysis was performed in serum and plasma samples.

#### **3.3.1 Control group**

Spot urine samples were collected from healthy Caucasian volunteers ( $n = 12$ ; 6 females and 6 males) and age-matched control (female, 40 – 63 years; male, 40 – 76 years). A urine samples was used from this control group for method validation. Urine samples from the volunteers were used to evaluate the applicability of the method for determination of TRP and its metabolites.

### 3.4. Biochemical analysis

Biochemical parameters were determined directly in serum, using the Prestige 24i automated analyzer (Cormay, Tokyo Boeki) and performed according to the manufacturer's instructions, as previously described (Costa *et al.* 2015). Serum concentrations of glucose, lipid profile (triglyceride, total cholesterol, HDL-c and LDL-c), creatinine, urea, uric acid, total bilirubin, ions (Ca<sup>2+</sup>, Na<sup>+</sup>, K<sup>+</sup>, and Cl<sup>-</sup>), enzymes (ALP, ALT, CK and LDH) and C-reactive protein were measured. Calibrations were performed for each parameter, with two appropriate calibrators, in order to plot a standard curve with 5 points. Enzyme activities were expressed as U/L, while others biochemical parameters were expressed as mg/dL, mg/L or mM/L in uniformity with the references. The estimated glomerular filtration rate (eGFR) was calculated using the formula:

$$\text{eGFR} = 141 * ([\text{creatinine}] / 0.9)^{-1.209} * (0.993)^{\text{age}}$$

The values were expressed as mL/min/1.73m<sup>2</sup>.

Plasma BNP levels were measured by enzyme-linked immunosorbent assay (EIA), using a commercial kit and performed according to the manufacturer's protocols. Data were processed and expressed as pg BNP/mL of plasma samples (Cowley *et al.* 2004).

### 3.5. Sample preparation for LC analysis

The 3-NT at final concentration of 2 µg/ml dissolved in 20 mM of ammonium formate in UPW (with 0.01% of formic acid) was used as internal standard (IS) and added to all samples.

### 3.5.1 Urine samples

For residues elimination of urine specimens obtained from patients and volunteers, samples were centrifuged at 6000 r.p.m. for 20 minutes at room temperature and stored at -20°C until analysis.

At the time of analysis, 1000 µL of urine aliquots were transferred to Eppendorf vials and centrifuged again at 13000 r.p.m. for 15 min at 4 °C and any suspended residue was disposed.

After that, 200 µL of urine were mixed with 50 µL of IS and 750 µL of mixture of standards at known concentration prepared in 20 mM of ammonium formate in UPW (with 0.01% of formic acid) for method validation or 750 µL of 20 mM of ammonium formate in UPW (with 0.01% of formic acid) to obtain the desired dilution of 1:5. The mixture was again centrifuged at 13000 r.p.m for 15 min at 4 °C to ensure correct homogenization.

Finally, sample was filtered through a filter of 22 µm pore size to ensure total freedom from particles that might impair the injection and 10 µL were analyzed by LC.

### 3.6. Optimization of the chromatographic conditions

During method optimization, mixtures of standard solutions were prepared in MeOH or 20 mM of ammonium formate in UPW (with 0.01% of formic acid). Different mobile phases, flow rates, oven temperature, injection volumes and wavelengths ( $\lambda$ , nm) were attempt (Table 2). The optimized conditions were achieved with a column oven temperature of 25°C, a flow rate of 0.7 mL/min and an injection volume of 10 µL. The FD was set to excitation and emission  $\lambda$  of 280 nm and 365 nm, respectively for TRP, coupled with an UV/VIS detector with a  $\lambda$  of 365 nm for KYN and 3-NT and 344 nm, for KA. Mobile phase consisted of 20 mM of ammonium formate in UPW (with 0.01 % of formic acid), ACN and EtOH (95/2/3, v/v/v). A  $\lambda$  program was used

for the UV/VIS detector: 0 to 17 min at 365 nm and from 17 to 40 min at 344 nm. The analysis was carried out in a total run time of 40 min.

**Table 2. Experimental conditions tested for the optimization of the separation of TRP, KYN, 3-NT and KA.**

	Mobile phase	$\lambda$ UV (nm)	$\lambda_{ex}$ (nm)	$\lambda_{em}$ (nm)	Flow-rate (mL/min)	T °C	pH
1	0.01% TFA : ACN (90:10, v/v)	250	280	365	0.7		3
2	0.01% TFA : ACN (87:13, v/v)	250	280	365	0.7		3
3	0.01% TFA : ACN (88:12, v/v)	250	280	365	0.7	25	3
4	0.01% TFA : ACN (88:12, v/v)	250	280	365	0.8	25	3
5	10 mM ammonium formate with 0.01% Formic acid : ACN (87:13, v/v)	250	280	365	0.7	25	5
6	10 mM ammonium formate with 0.01% Formic acid : ACN (87:13, v/v)	250	280	365	0.8	25	5
7	20 mM ammonium formate with 0.01% Formic acid : ACN (87:13, v/v)	250	280	365	0.7	25	4,4
8	20 mM ammonium formate with 0.01% Formic acid : ACN (90:10, v/v)	250	280	365	0.7	25	4,4
9	20 mM ammonium formate with 0.01% Formic acid : ACN (91:9, v/v)	250	280	365	0.7	25	4,4
10	20 mM ammonium formate with 0.01% Formic acid : EtOH (91:9, v/v)	250	280	365	0.7	25	4,4
11	20 mM ammonium formate with 0.01% Formic acid : ACN (95:5, v/v)	250	280	365	0.7	25	4,4
12	20 mM ammonium formate with 0.01% Formic acid : ACN (95:5, v/v)	250	280	365	0.8	25	4,4
13	20 mM ammonium formate with 0.01% Formic acid : ACN: EtOH (95:3:2, v/v/v)	250	280	365	0.8	25	4,4
14	20 mM ammonium formate with	250	280	365	0.7	25	4,4

	0.01% Formic acid : ACN: EtOH (95:2:3 v/v/v)						
15	20 mM ammonium formate with 0.01% Formic acid : ACN: EtOH (95:2:3 v/v/v)	250	280	365	0.8	25	4.4
16	20 mM ammonium formate with 0.01% Formic acid : ACN: EtOH (95:2:3 v/v/v)	365	280	365	0.8	25	4.4
17	20 mM ammonium formate with 0.01% Formic acid : ACN: EtOH (95:2:3 v/v/v)	344	280	365	0.7	25	4.4
18	20 mM ammonium formate with 0.01% Formic acid : MeOH : EtOH (95:2:3 v/v/v)	365	280	365	0.7	25	4.4
19	20 mM ammonium formate with 0.01% Formic acid : ACN: EtOH (95:2:3 v/v/v)	365/ 344	280	365	0.7	25	4.4

ACN: Acetonitrile; EtOH; Ethanol; MeOH: Methanol; TFA: trifluoroacetic acid

### **3.7. Method validation**

Method validation was performed according to the European Medicines Agency guidelines (EMA) (EMA, 2011) considering the following parameters: selectivity, linearity, accuracy, intra and inter-day precision, recovery, limit of quantification (LOQ) and limit of detection (LOD).

#### ***Selectivity***

Selectivity was evaluated by comparing the chromatograms of six different urine samples with the chromatograms of urine samples spiked with the target compounds and with a chromatogram of a standard mixture. The samples were injected after being prepared as described above.



### *Linearity*

Linearity was studied using matrix-matched calibration by spiking urine samples with seven different concentrations in triplicate prepared in 20 mM of ammonium formate in UPW (with 0.01% of formic acid). The range of nominal concentrations can be found in Table 3.

Since selected analytes are endogenous compounds, blank urine samples, i.e., unspiked urine samples were used.

The calibration curves were obtained after subtraction of a urine sample not spiked (blank samples). Equations were obtained after least-squares linear regression of the ratio analyte / IS. The calibration curve linearity was evaluated by its correlation coefficient ( $r^2$ ).

**Table 3. Range of nominal concentrations (ng/mL) of the standards used for the calibration curve.**

	TRP ng/mL	KYN ng/mL	KA ng/mL
Calibration curve concentrations	100	50	125
	136	75	250
	275	100	500
	338	200	675
	563	338	900
	675	400	1000
	1100	600	1500

### *Accuracy and precision*

Accuracy, intra- and inter-batch precision were determined by analysis in three replicates of three quality control standard solutions (QC) at three different concentrations within the linearity range (Table 4). Accuracy was expressed as the percentage of agreement between the determined value obtained by the method and the nominal value. Precision (inter and intra-day) was expressed as the percentage of relative standard deviation (% RSD). QCs were always analyzed

together with their blank samples. The spike concentration was calculated by subtracting the concentration obtained for the unspiked sample (blank) to the one of the QC.

**Table 4. Quality control nominal concentrations.**

	TRP ng/mL	KYN ng/mL	KA ng/mL
QC	200	150	375
	550	300	750
	900	500	1200

QC: Quality control

### ***Recovery***

The recovery was calculated by the ratio (analyte / IS) in urine in the same concentration of the QC and ratio (analyte / IS) prepared in 20 mM of ammonium formate in UPW (with 0.01% of formic acid). The value was expressed as a percentage. The spike concentration was calculated by subtracting the concentration obtained for the unspiked sample to the one of the QC.

### ***Limit of quantification (LOQ) and Limit of detection (LOD)***

The LOQ and LOD were calculated using the mathematic formula:

$$LOQ = 10 \times (s / S), LOD = 3.3 \times (s / S)$$

Where, *s* is the standard deviation of y-intercepts, and *S* the slope of the calibration curve.

### ***Application to urine samples***

To calculate the analyte concentrations in the urine samples from HF patient and healthy volunteers, the analyte / IS ratio was determined.

### **3.8. Statistical analysis**

All demographic and clinical variables used for characterization of HF patients were obtained from both male and female patients, whereas for biological variables only male patients were used. Analysis of blood and urine data from men patients was stratified in 2 groups according to the presence of type 2 diabetes mellitus (DM2/HF) or absence (HF). Data were expressed as means  $\pm$  standard deviation (SD) minimums and maximums, or percentages, whereas TRP and its metabolites data were expressed as median and interquartile range (difference between the first and third quartiles Q1 and Q3 respectively). The ratios presented were calculated by dividing the concentration of one substrate by the other (e.g. LDL-c/HDL-c ratio, KYN/TRP ratio and KA/KYN ratio). All statistical analyses were carried using SPSS (Statistical Package for the Social Sciences) version 25 for windows (Chicago, USA). One-way analysis of variance (ANOVA), non-parametric tests between independent groups Mann-Whitney U test where it was found that the distribution of the figures between the two groups has the same form, and the Student *t* test between independent groups were used to determine differences between the means or median of diabetic and non-diabetic groups. Statistically significance differences were considered when the *p* value was less than 0.05.

## 4. RESULTS AND DISCUSSION

The enhance of TRP catabolism induced by inflammatory states has been implicated in cardiovascular pathology (Song *et al.* 2017), suggesting that an imbalance of kynurenine pathway with a shifted toward generate prooxidant metabolites might be exacerbated in CVD patients. Therefore, a reliable non-invasive method for quantification of these metabolites in biological matrices was developed, validated and applied to urine samples of cardiac patients of "Heart&Mind" study. In addition, descriptive characteristics of the study population were provided and evaluated. The results of biological samples analysis were further categorized using the demographic and clinical data.

### 4.1. Patients characteristics

Mean age was  $62 \pm 9$  years (age range between 42 and 77 years) and 86% of participants were male. Male and female patient characteristics were evaluated and summarized in Table 5. Due to demographic heterogeneity of the patients a cut-off value of 65 years old was applied to discriminate elderly from adult group. It was identified that 36% ( $n = 8$ ) of the participants were older (data not shown). Despite the knowledge that age is a risk factors for HF (Bui *et al.* 2011) and it may influence the kynurenine pathway activity (Badawy 2020) in the present study the effect of age was not evaluated.

All patients had ventricular EF less than 40% (an average of 25.8%), which is classified as HF with reduced EF (HFrEF) (Lepojärvi *et al.* 2018). With respect to the anthropometric parameters, mean body weight was 75 kg, values were in a long-range (between 44 and 107 kg) and BMI average of  $27 \text{ Kg/m}^2$ , giving an indication that was an overweight population. However, when BMI cut-off points of WHO were used (data not shown), the results showed that 18% had overweight and 38% were obese, while the remaining had BMI within normal (40%) and underweight (5%) values (data not shown). The abdominal perimeter, which is considered as another great predictor of heart disease (Nicklas *et al.* 2006), was determined and the

results on abdominal circumference showed a mean ( $\pm$  standard deviation) of 97 cm ( $\pm$  11 cm). The recommendations are values less than 88 cm for female and less than 94 cm for men (Nicklas *et al.* 2006), which indicated that participants of the present study presented a metabolic risk for heart disease.

The recent developments on the link between metabolic risk factors and HF are issue of debate. Indeed, body weight above the normal for age and sex as a predictor of mortality has not yet reached a unanimous conclusion and the controversy arisen by the so called 'obesity paradox'. Moreover, recent epidemiological studies showed that overweight was associated with significantly lower all-cause mortality (Flegal *et al.* 2013) and can be an protect factor for HF disease (Clark *et al.* 2014).

Mean systolic blood pressure (SBP) and diastolic blood pressure (DBP) were  $115 \pm 13$  and  $68 \pm 11$  mmHg, respectively. The blood pressure guidelines considers normal values of SBP < 120 mm Hg and DBP < 80 mm Hg (Fu 2015; Ortiz Galeano *et al.* 2019). Therefore, patients of the present study showed lower values than the recommended upper limit, which can be an effect of the antihypertensive medication. Considering health-related habits, 46% of patients reported had no physical activity. Regarding others cardiovascular risk recorded in medical history, patients presented DM2 (36%), dyslipidemia (19%) and hypertension (14%). Among the patients with diagnosis of DM2, 86% were males and 14% were female (data not shown). All patients were under medical treatment, an average of 7 drugs/patient/day, which included diuretics (82%), beta blockers (77%), angiotensin inhibitors (55%), statins (55%), antiarrhythmic (50%), antiplatelet (46%), uricosuric (32%) and antidiabetic (22%) medication.

**Table 5. Characteristics from all patients.**

	n (%)	Mean ± SD	[Min.-Max.]
<b>Demographic and clinical</b>			
Male gender	19 (86)	-	-
Female gender	3 (14)	-	-
Age, years	-	62 ± 9	42 - 77
Weight, kg	-	75 ± 15	45 - 107
Abdominal circumference, cm	-	97 ± 11	78 - 117
BMI, Kg/m <sup>2</sup>	-	27 ± 5	17 - 41
SBP, mmHg	-	115 ± 13	91 - 143
DBP, mmHg	-	68 ± 11	45 - 89
Heart rate, b.p.m.	-	65 ± 10	53 - 95
Ventricular EF, %	-	25 ± 8	14 - 38
<b>Cardiovascular risk factors</b>			
Hypertension	3 (14)	-	-
DM2	8 (36)	-	-
Dyslipidemia	4 (19)	-	-
Obesity	8 (36)	-	-
Current smoker	1 (5)	-	-
No physical activity	10 (46)	-	-
<b>Medication</b>			
Antiplatelet	10 (46)	-	-
Statins	12 (55)	-	-
Angiotensin inhibitors	12 (55)	-	-
Beta blockers	17 (77)	-	-
Antiarrhythmic	11 (50)	-	-
Proton-pump inhibitor	8 (36)	-	-
Diuretics	18 (82)	-	-
Antidiabetics	6 (22)	-	-
Uricosuric	7 (32)	-	-
Anxiolytics / Benzodiazepines	4 (18)	-	-
Others	13 (59)	-	-

Values are expressed as n (%) or mean ± SD. BMI: body mass index; b.p.m.: beats/min; DBP: diastolic blood pressure; DM2: type 2 diabetes mellitus; EF: ejection fraction, SBP: systolic blood pressure

Male patients (n = 19) were further stratified into two groups diabetic (DM2/HF) and non-diabetic (HF) and their characteristics were summarized in Table 6. Mean abdominal circumference and body weight were higher in DM2/HF without significant difference between mean values. Using BMI cut-off points (data not shown), 50% of diabetic patients had obesity, 33% had normal weight and 16% had overweight; while in the non-diabetic group, 62% had normal weight, 31% were obese and 8% had overweight. There is no significant difference for blood pressure and heart rate between patients groups, however DM2/HF patients had slightly higher SBP and heart rate values compared with non-diabetic HF patients.

**Table 6. Male patient characteristics.**

Variables	HF (n =13)	DM2/HF (n =6)	<i>p</i> value
Weight, kg	72 ± 17	81 ± 10	0.44
Abdominal circumference, cm	95 ± 11	101 ± 12	0.18
BMI, Kg/m <sup>2</sup>	27 ± 6	29 ± 3	0.37
SBP, mmHg	112 ± 12	122 ± 5	0.24
DBP, mmHg	68 ± 12	66 ± 5	0.78
Heart rate, b.p.m.	64 ± 11	66 ± 6	0.62
Ventricular EF, %	26 ± 9	22 ± 4	0.51

Values are expressed as n (%) or mean ± SD. BMI: body mass index; b.p.m.: beats/min; DBP: diastolic blood pressure; DM2: type 2 diabetes mellitus; EF: ejection fraction; SBP: systolic blood pressure.

## 4. 2. Biochemical parameters

All biochemical parameters were analyzed in serum samples from male and female patients. However, data obtained from female group were excluded from statistical analysis, since the number was not significant to evaluate the difference inherent to gender. Therefore, Table 7 presents the biochemical data from male patients that was also stratified by diabetic (DM2/HF) and non-diabetic (HF) groups.

Serum concentration of creatinine, urea, eGFR, total cholesterol, LDL-c and LDL-c/HDL-c ratio were significantly different between DM2/HF and HF with *p value* < 0.05, whereas, uric acid, total bilirubin, triglyceride, HDL-c, glucose, ions, enzymes, BNP and C-reactive protein levels did not differ between groups.

Mean creatinine and urea levels were higher in DM2/HF, while the mean eGFR value was lower when compared with HF patients. Moreover, serum creatinine and urea concentration in DM2/HF group were also above the reference values for creatinine (0.7 mg/dL to 1.2 mg/dL) (Wu *et al.* 2016) and urea (15 mg/dL to 39 mg/dL) (de Almeida *et al.* 2016). In addition, mean eGFR value in DM2/HF group was below the normal reference value, which is  $\geq 90$  mL/min/1.73m<sup>2</sup> (Çelik *et al.* 2018). These biochemical parameters are widely used to evaluate renal function and can be impaired in HF patients as well as in diabetic patients (Damman and Testani 2015; Lehrke and Marx 2017). Urea is considered a urinary toxin (Lau and Vaziri 2017), which can causes an increase in oxidative stress and endothelial dysfunction, being both mechanisms associated with cardiac disease (Assem *et al.* 2018). Therefore, the present results showed altered renal biomarkers in HF patients with diabetes, suggesting a compromised renal function.

As it was expected, glucose levels were higher in DM2/HF patients ( $171 \pm 71$  mg/dL) compared with non-diabetic group ( $113 \pm 26$  mg/dL). Moreover, both groups had mean values above de normal range for fasting blood glucose (between 72 to 99 mg/dL) (Dimova *et al.* 2017).

Regarding the lipid profile, total cholesterol and LDL-c were lower in the DM2/HF group compared to HF patients and, despite this difference, the lipid profile of both groups were within the reference values for total cholesterol < 200 mg/dL (Wagner



*et al.* 2019) and LDL-c < 100 mg/dL (McCormack *et al.* 2016). It is important to mention that 55% of these patients take statins therapy, which is the most commonly prescribed medications for decreasing lipid levels (Costa *et al.* 2016). Although total cholesterol is not a specific indicator of cardiac disease, LDL-c is quite important since its oxidized species is a risk factor for increased inflammation (McCormack *et al.* 2016). For LDL-c, the HF patients had a higher level ( $90 \pm 34$  mg/dL) compared with DM2/HF had lower levels ( $52 \pm 24$  mg/dL). Even during statins therapy, HDL-c levels are considered as a strong inverse predictor of cardiovascular events (Barter *et al.* 2007) and levels above 40 mg/dL are recommended (de Souza *et al.* 2009). However, both patient groups showed low levels of HDL-c when compared with reference values and without differences between HF and DM2/HF groups. The results obtained in the present study showed differences between groups for LDL-c/HDL-c ratio, which is known as another strong predictor of cardiac disease (Kunutsor *et al.* 2017). This ratio was significantly higher in the HF patients (~4) when compared with DM2/HF group (~3). Finally, there were no differences between groups in triglycerides levels and the concentrations were within reference value (< 150 mg/dL) (Kopin and Lowenstein 2017).

For evaluation of hepatic injury, several markers were quantified, namely total bilirubin, LDH, ALP, ALT and AST levels (Table 7). Despite, not statistically different the enzymes levels, HF patients showed higher LDH levels and lower ALP levels compared DM2/HF group patients. The LDH concentration was also higher than reference values, which can indicate injury in tissues such as the heart, liver or kidneys (Li *et al.* 2009). However, ALP levels of both groups were within the normal reference ranges, between 40 and 130 U/L (Clark *et al.* 2003). Regarding ALT levels, HF patients were higher mean than DM2/HF group, although values of both groups were within the normal reference value for ATL < 41 U/L (Galvin *et al.* 2015). The quantification of AST was similar in mean values between groups, but both were below the normal reference limit for AST < 45 U/L (Peng *et al.* 2016). For total bilirubin concentration, the mean values were also similar between groups.

C-reactive protein is considered an inflammatory biomarker, which is produced by the liver and is found in higher concentrations during inflammatory states of the body (Black *et al.* 2004). In the present study, C-reactive protein mean levels were slightly higher in the DM2/HF group (3.7 mg/L) compared to HF group (2.7 mg/L) but without significant differences in this inflammatory marker. However, the results obtained for C-reactive protein suggested that all patients showed a low-grade of inflammation. Indeed, it is considered that a mild increase of C-reactive protein levels (values between 2 mg/L and 10 mg/L) may indicated a metabolic inflammatory state (Markanday 2015).

**Table 7. Biochemical data of male patients.**

PARAMETERS	HF (n =13 )	DM2/HF (n =6 )	<i>p</i> value
Creatinine, mg/dL	0.7 ± 0.4	1.5 ± 0.4	<0.05
Uric acid, mg/dL	8.3 ± 2.6	6.5 ± 2.4	0.52
Urea, mg/dL	44.6 ± 14.1	62.8 ± 20.4	<0.05
eGFR, mL/min/1,73m <sup>2</sup>	136 ± 64	72 ± 8	<0.05
Na <sup>+</sup> , mM/L	69.8 ± 11.4	65.5 ± 16.5	0.64
Mg <sup>2+</sup> , mg/dL	2.1 ± 0.4	1.9 ± 0.4	0.61
Ca <sup>2+</sup> , mg/dL	8.1 ± 1.4	8.0 ± 2.2	0.92
Cl <sup>-</sup> , mM/L	100 ± 14	93 ± 12	0.37
Total bilirubin, mg/dL	0.3 ± 0.2	0.3 ± 0.3	0.81
LDH, U/L	442 ± 378	371 ± 73	0.76
ALT, U/L	8.6 ± 11.4	4.1 ± 4.7	0.24
AST, U/L	16.6 ± 6.3	16.8 ± 3.3	0.86
ALP, U/L	53 ± 20	73 ± 27	0.19
C-reactive protein, mg/L	2.7 ± 4.0	3.7 ± 3.0	0.33
BNP, pg/mL	236 ± 52	210 ± 41	0.08
CK, U/L	50 ± 26	61 ± 43	0.57

Glucose, mg/mL	113 ± 26	171 ± 72	0.06
Total cholesterol, mg/dL	167 ± 35	130 ± 19	<0.05
LDL-c, mg/dL	90 ± 34	52 ± 24	<0.05
HDL-c, mg/dL	25 ± 6	20 ± 8	0.30
Triglycerides, mg/dL	149 ± 62	115 ± 20	0.27
LDL-c/HDL-c ratio	4 ± 1	3 ± 1	<0.05

Values are expressed as mean ± SD. ALP: alkaline phosphatase; ALT: alanine aminotransferase; AST: aspartate aminotransferase; BNP: brain natriuretic peptide; CK: creatine kinase; eGFR: estimated glomerular filtration rate; LDH: dehydrated lactate; HDL-c: high-density lipoprotein cholesterol; LDL-c: low-density lipoprotein cholesterol.

Regarding the cardiac biomarker, BNP, the mean plasma levels were higher in the HF group, but not statistically different between groups, nevertheless both means were above normal reference values for BNP < 100 pg/mL (Table 7) (Rocca and wijk 2019). Increase in plasma BNP concentrations is associated with left ventricular dysfunction (Gölbapý *et al.* 2004) and hypertension (Kato *et al.* 2017). The present study showed that non-diabetic HF patients had the high mean value for BNP (236 pg/mL) compared with DM2/HF group (210 pg/mL).

It has been demonstrated that a decrease in CK serum levels in cardiac patients is associated with a decrease in ventricular function, namely EF (Fowler *et al.* 2015). In addition, CK is known to be an enzyme involved in the production of energy in the form of ATP (McLeish *et al.* 2005), therefore, the present study performed the quantification of serum CK concentrations. The results obtained showed that mean CK levels were slightly higher in the DM2/HF group (61 U/L) compared with mean levels found in HF group (50 U/L) (Table 7).

Uric acid is a biochemical parameter that gives an indication of the renal status of patients and is also considered a predictor of heart disease (Wu *et al.* 2016). HF patients presented higher mean levels for uric acid (8.3 mg/dL) than DM2/HF group (6.5 mg/dL). Moreover, mean concentration in patients was above the uric acid reference range values (3.5 mg/dL to 7.0 mg/dL) (Ndrepapa 2018). However, uric acid levels were not statistically different between patient groups, result that can be

explained by a strongly influence of diuretic therapy, since 82% of all patients use these drugs and 46% of them use more than one type of diuretics (Reyes 2003). It should also be noted that 50% of DM2/HF patients use uricosuric medication, while only 23% of patients of HF patients (data not shown) use this type of drugs, this factor can explain the values obtained by both groups (Goicoechea *et al.* 2010).

The results of quantifications of serum levels of ions, namely Na<sup>+</sup>, Mg<sup>2+</sup>, Ca<sup>2+</sup> and Cl<sup>-</sup> were not different between both groups. However, it was found that the concentration of some ions tends to be different among patient groups and/or reference limits. In HF group, the mean Na<sup>+</sup> concentration was 69.8 mM/L, while DM2/HF patients presented a slightly lower concentration of 65.5 mM/L (Table 7). Moreover, mean value in both groups were below normal levels for Na<sup>+</sup> (> 135 mM/L), suggesting the presence of an hyponatremia, a very common condition of cardiac patients (Palazzuoli *et al.* 2017; Mahmood *et al.* 2019). Hyponatremia can be a consequence of several situations (Mahmood *et al.* 2019). Among others, it has been associated with a decrease of blood volume in circulation, that leads to the activation of the sympathetic nervous system and renin-angiotensin-aldosterone system, causing the release of vasopressin (Mahmood *et al.* 2019). These pathways activation is very frequent in patients HFrEF (Mahmood *et al.* 2019), which was the diagnosis of all patients participants in our study. Corroborating previous studies (Tuba *et al.* 2019), our results showed that Na<sup>+</sup> levels were lower in HFrEF patients, indicating that hyponatremia can be present in both diabetic and non-diabetic HF patients. Only in HF patients, Cl<sup>-</sup> concentrations were below the normal reference value (> 96 mM/L) (Laecke 2019), results that are in accordance with previous studies (Grodin *et al.* 2018). Others ions concentration quantified in both groups were within reference values for Mg<sup>2+</sup> (Laecke 2019) and Ca<sup>2+</sup> levels (Shrimanker and Bhattarai 2020).

### 4.3. Optimization of urine sample preparation procedure

Urine sample preparation procedure was optimized in order to achieve the expected concentration of target compounds in urine samples from patients and to eliminate the majority of the interferences (Table 1S, SM).

Therefore, initially, only one centrifugation was made during 15 min at 13,000 r.p.m. at 4 °C to eliminate interferences that could precipitate into the column or interfere with compounds detection. Nevertheless, this procedure shown to be insufficient. Thus, urine samples were diluted 10x and 5x, to find the most adequate dilution factor (DF). The dilution was made with 0.01% of trifluoroacetic acid (TFA) in UPW at pH 3. Nevertheless, this procedure was still not efficient, i.e., not able to quantify the selected compounds due to interferences.

Thus, two centrifuges were performed. Urine samples were centrifuged at 13,000 r.p.m. during 15 min at 4 °C and then diluted with 0.01% of TFA in UPW at pH 3 to achieve a 10x or 5x DF and again centrifuged 15 min at 13,000 r.p.m. at 4 °C. The better results were found for a 5x dilution since it led to a greater recovery of the TRP and the metabolites under study.

Nevertheless, to improve the sensitivity of the method, the dilution was done with mobile phase, i.e., with 20 mM of ammonium formate in UPW (with 0.01% of formic acid) at pH 4.4. Two different DF were also tested, 5x and 10x. The supernatant was collected and filtered with a 0.22 µm pore size filter to avoid any precipitation in the column. This procedure allowed the recovery of all compounds. Nevertheless, still to improve sensitivity and to eliminate interferences two other sample preparations procedures were tested: first an aliquot of 200 µl of urine was evaporated and reconstituted in the same volume of 20 mM of ammonium formate in UPW (with 0.01% of formic acid) pH 4.4 and then filtered with a 0.22 µm pore size filter. Second, an aliquot of 200 µl of urine was evaporated and reconstituted in 100 µl of 20 mM of ammonium formate in UPW (with 0.01% of formic acid) pH 4.4 and filtered with a 0.22 µm pore size filter. Both procedures resulted in an increase of the interferences signal and therefore the most efficient sample preparation process consists in the centrifugation during 15 min at 13,000 r.p.m. at 4 °C of the

urine and then dilution of 200  $\mu$ l of urine with 800  $\mu$ l of 20 mM of ammonium formate UPW (with 0.01% of formic acid) pH 4.4 to achieve a DF of 5 and finally filtered with a 22  $\mu$ m pore size filter before LC analysis.

#### **4.4. Optimization of the chromatographic conditions**

The chromatographic conditions were optimized in order to achieve the separation of analytes of interest and eliminate the interferences.

All conditions tested were performed using a column Luna® 3  $\mu$ m PFP (2) 100<sup>a</sup> from Phenomenex. The variables used to adjust the method were: type of acid, the proportions and types of organic solvent, oven temperature (T), flow rate and different  $\lambda$  for the UV-Vis and FD.

The first conditions tested were with a mobile phase consisting of 0.01% TFA : ACN (90:10, v/v) and (87:13, v/v) at pH 3 with a flow rate of 0.7 ml/min. With these conditions separation of all compounds was not achieved. The  $\lambda$  (nm) was set at 250 nm for the UV-VIS detector for KYN, 3-NT and KA and at 280 and 365 nm for FD detector at the  $\lambda$  excitation and emission, respectively for TRP.

After this, mobile phase was change to 0.01% TFA : ACN (88:12) at pH 3 and two different flows rate were tested, 0.7 mL/min and 0.8 mL/min. Further, T was fixed to 25°C using the column oven.

Although these two conditions allowed the separation of all the analytes under study, retention time (RT) of the analytes were not reproducible among injections and new mobile phases/ conditions were attempt (Figure 2 and 3).

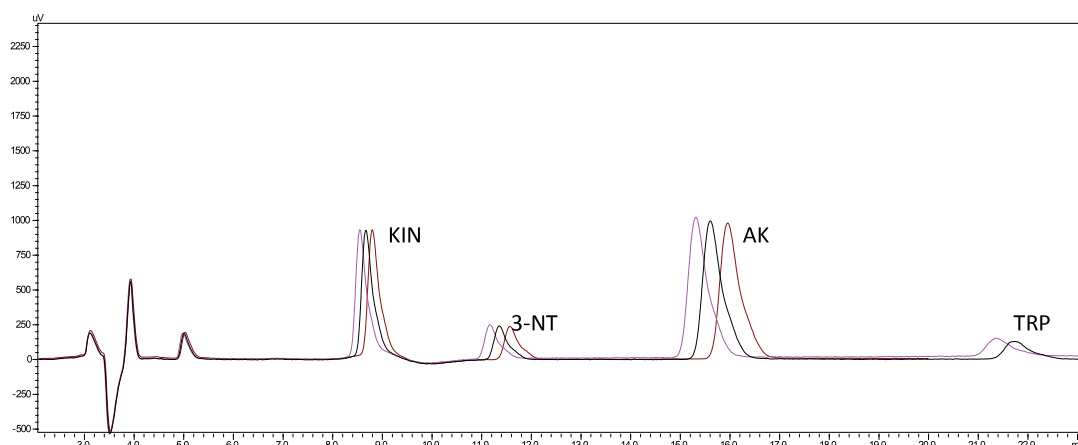


Figure 2 : Chromatogram showing the non-reproducibility of the RT using the UV-VIS detector with the mobile phase of 0.01% TFA : ACN (88:12, v/v) at concentration of 500 ng/mL ( $\lambda$  exc/em = 280/365 nm (FD);  $\lambda$  = 250 nm (UV-Vis)).

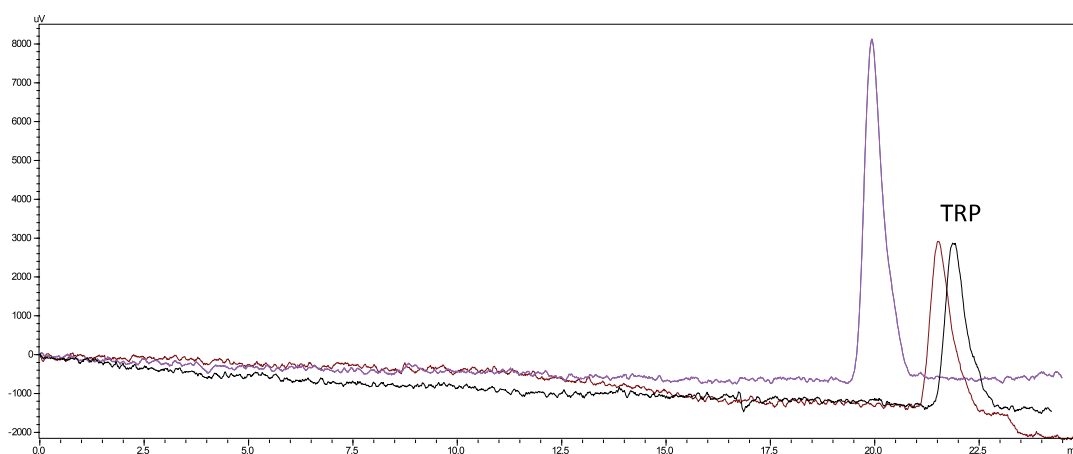
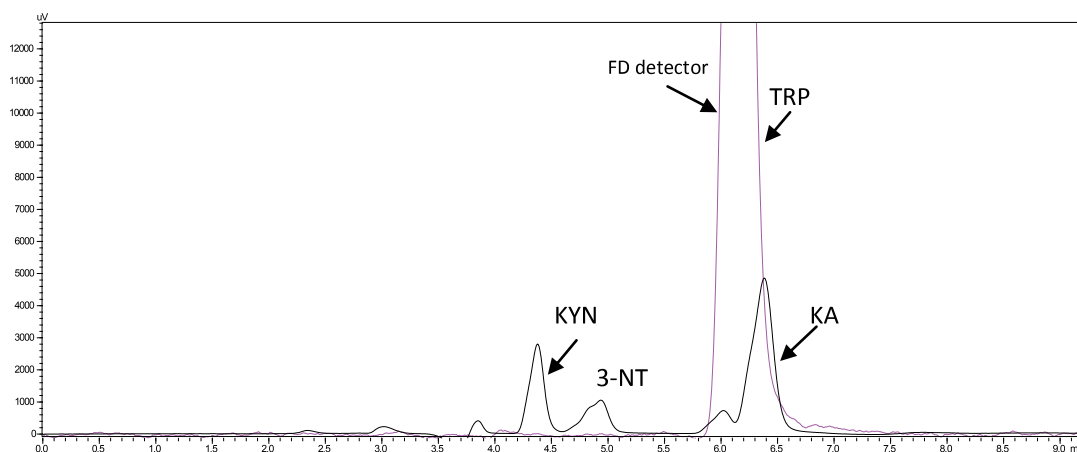


Figure 3. Chromatogram showing the non-reproducibility of the RT using the FD detector with the mobile phase of 0.01% TFA : ACN (88:12, v/v) at concentration of 500 ng/mL ( $\lambda$  exc/em = 280/365 nm (FD);  $\lambda$  = 250 nm (UV-Vis)).

Thus, 0.01% TFA was substituted by 10 mM and 20 mM ammonium formate in UPW with 0.01% of formic acid. A mobile phase composed by 20 mM ammonium formate in UPW with 0.01% of formic acid : ACN at pH 4.4 (87:13, v/v), enabled the reproducibility of RT. Other parameters were changed to improve separation namely flows rates (0.7 and 0.8 mL/min) and T at 25°C. With these conditions, poor separation of the compounds was achieved (Figure 4).



**Figure 4.** Chromatogram of a mixture of the compounds at 500 ng/mL using a mobile phase of 20 mM ammonium formate in UPW with 0.01% formic acid : ACN (87:13, v/v) at pH 4.4 showing the compounds overlap (black line: UV-Vis; pink line: FD;  $\lambda_{exc}/em = 280/365$  nm (FD);  $\lambda = 250$  nm (UV-Vis)).

Thus, other mobile phase proportions were tested using 20 mM ammonium formate UPW with 0.01% of formic acid: ACN at pH 4.4 of (90:10, v/v), (91:9, v/v) and (95:5, v/v) at a flow rate of 0.700 ml/min and at 25°C. In all cases, RT of KYN was similar to the IS (3-NT) which caused the two compounds to outspread and overlap (data not shown).

To delay the RT and improve separation, the ACN was replaced by EtOH. This new mobile phase of 20 mM ammonium formate in UPW with 0.01% of formic acid : EtOH (91:9, v/v) at pH 4.4, flow rate 0.700 mL/min and 25°C lead to the separation of KYN but caused an enlargement of the peaks for 3-NT, TRP and KA (Figure 5).



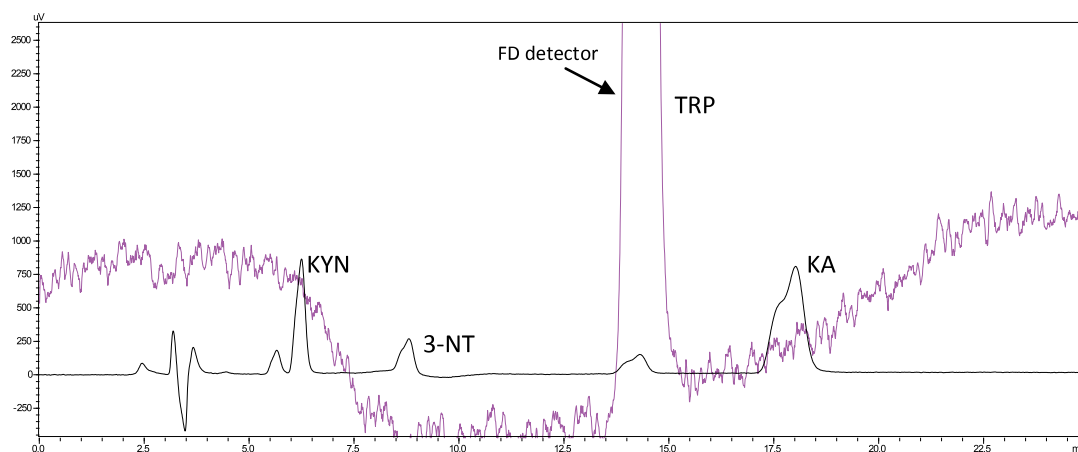


**Figure 5.** Chromatogram of a mixture of the compounds at 500 ng/mL using a mobile phase of 20 mM ammonium formate in UPW with 0.01% formic acid : EtOH (91:9, v/v) at pH 4.4 showing the enlargement of the peaks of 3-NT, TRP and KA. (black line: UV-Vis detector; pink line: FD);  $\lambda_{exc/em} = 280/365$  nm (FD);  $\lambda = 250$ nm (UV-Vis).

Thus, a new mobile phase, consisting in a mixture of three solvents was tested, 20 mM ammonium formate in UPW with 0.01% of formic acid, ACN and EtOH at two different proportions (91:2:3, v/v/v) and (91:3:2, v/v/v) at a flow rate of 0.8 mL/min pH 4.4 and T of 25°C. Also, the proportions (95:2:3, v/v/v) (Figure 6) and (95:3:2, v/v/v), at a flow rate 0.7 mL/min and T of 25°C were tested. All conditions allowed resolution of all compounds however, when applied to the urine samples, other matrices interferents overlaid compounds of interest (Figure 7).

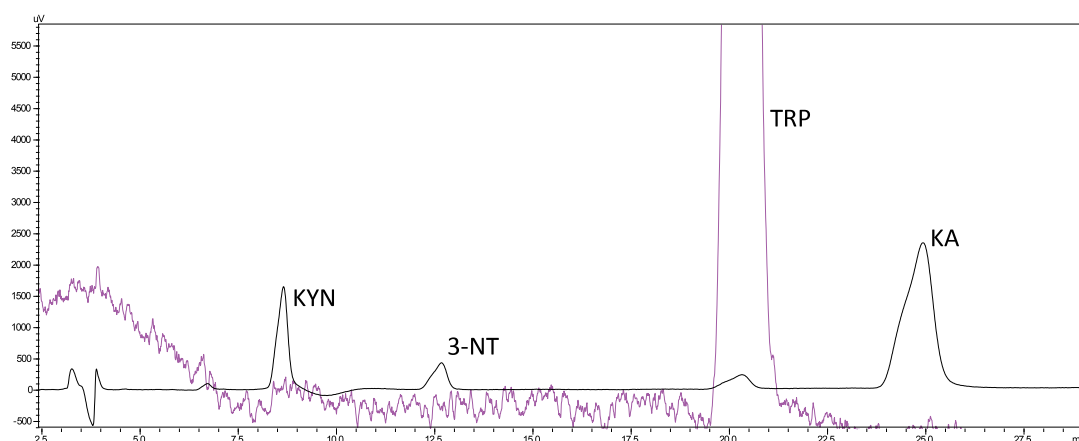


**Figure 6.** Chromatogram of a mixture of the compounds at 1 µg/mL using a mobile phase of 20 mM ammonium formate with 0.01% formic acid : ACN: EtOH (95:2:3, v/v/v) at a flow rate of 0.800 mL/min at  $\lambda$  250 nm UV-VIS detector and at  $\lambda$  exc/em= 280/365 nm for the FD detector (black line: UV-VIS detector; pink line: FD)

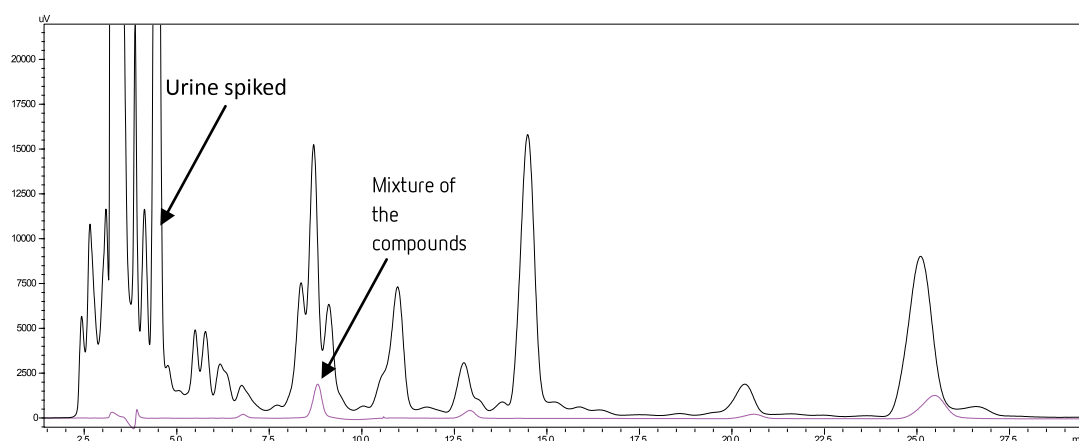


**Figure 7.** Chromatogram of urine spiked with standard of 10 µg/mL overlapping a chromatogram of a mixture of the compounds at 1 µg/mL. (black line: urine spiked; pink line: mixture of analytes;  $\lambda$ exc/em = 280/365 nm (FD);  $\lambda$  = 250nm (UV-Vis).

To eliminate matrices interferences, a  $\lambda$  program for the UV-VIS detector was performed. Finally, the conditions that allowed resolution of the compounds of interest and without interferences of the matrices were: 20 mM ammonium formate in UPW with 0.01% of formic acid : ACN : EtOH (95:2:3, v/v/v) pH 4.4, at a flow rate of 0.7 mL/min, a T of 25°C and a  $\lambda$  program for UV-VIS detector was established:

from 0 to 17 min at 365 nm and from 17min to 40 min at 344 nm and for the FD at 280 nm and 365nm for excitation and emission, respectively (Figure 8 and 9).

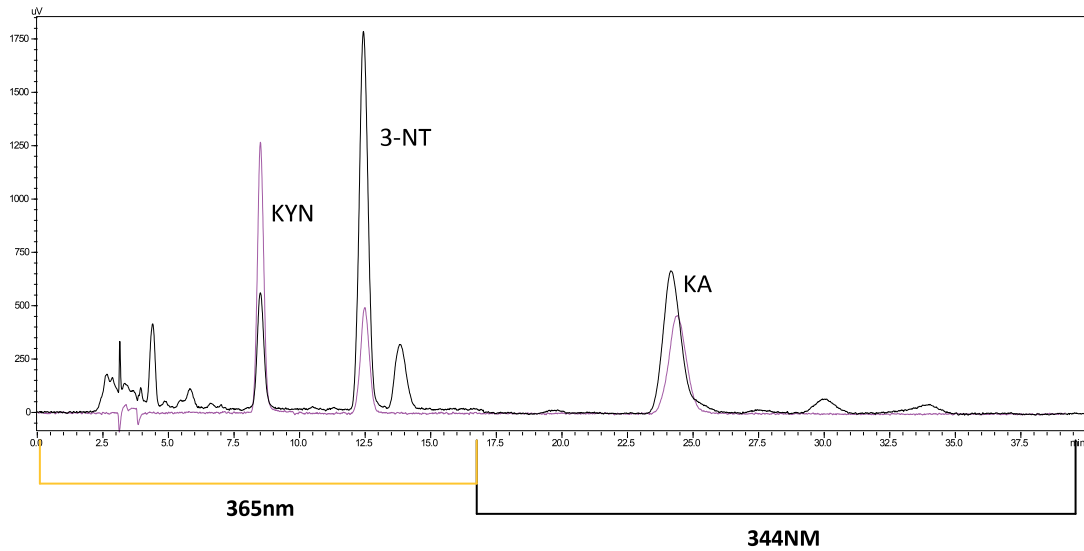


Figure 8. Chromatogram of 5x diluted patient urine sample overlapping a standard of 1 µg/mL with a UV-VIS detector set at 0 to 17 min at 344 nm and from 17 to 40 min at 365 nm (black line: urine patient sample; pink line: standard mixture).

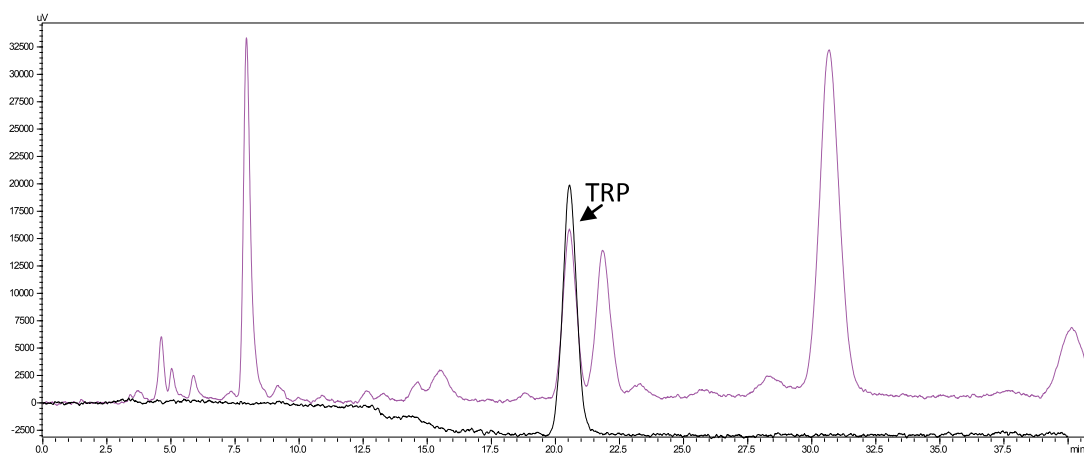


Figure 9. Chromatogram of 5x diluted patient urine sample overlapping a standard of 1 µg/mL with a FD detector set at 280 nm and 365nm for excitation and emission (black line: urine patient sample; pink line: standard mixture)

RT of KYN, 3-NT, KA and TRP were 8.8, 12.7, 24.5 and 20.6 min, respectively.

### *Method validation*

The method was validated according to international guidelines established by EMA considering selectivity, linearity, accuracy, precision, recovery, LOQ and LOD. As all the compounds are endogenous, and thus present in all urine samples matrices it was not possible to obtain an analyte-free urine sample for conducting the validation experiments. Thus, a blank matrix was used for method validation.

### *Selectivity*

Selectivity corresponds to the ability of the method to identify and quantify the analytes of interest unequivocally in the presence of other analytes and/or impurities. Selectivity of the method was verified by comparison of the chromatograms with the mixture of standards in 20 mM ammonium formate in UPW with 0.01% of formic acid, a urine sample and spiked urine sample.

For that, six urine samples of healthy volunteers were analyzed. Each urine sample from volunteer was analyzed without and after spiking of a mixture of standards.

No interferences were found at the same RT of the analytes in the optimized conditions allowing the validation and applicability of the method for the quantification of the analytes (Figure 10).

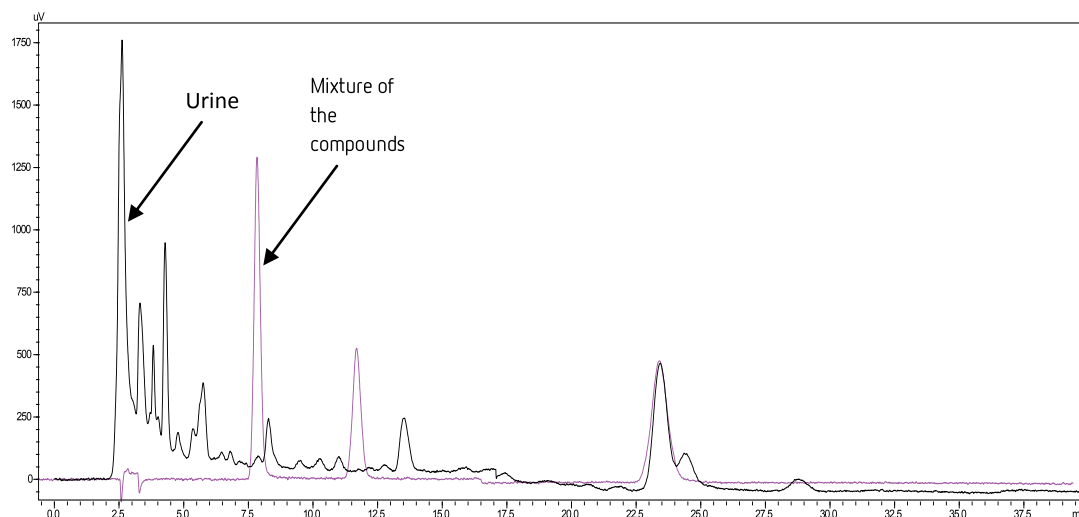


**Figure 10. Chromatogram of 5 x diluted urine sample from a healthy volunteer with overlapped with 1  $\mu\text{g}/\text{mL}$  standard mixture** (Black line: urine sample from healthy volunteer; pink line: mixture of the analytes)

### *Linearity*

Linearity was obtained after spiking the 5x diluted urine sample at 7 different and known concentrations, including the LOQ of each compound which was used as the starting point of each of the curves (Table 8). Each concentration was prepared in triplicate and injected in triplicate.

The ratio between the area of the metabolite of interest (KYN, TRP and KA) and the area of the IS (3-NT) in each mixture was determined. From the ratio found, the unspiked blank matrix ratio was subtracted to build the calibration curve with the exact value of compound of interest. The calibration curves for each analyte, as well as the linear regression equations and respective LOQ and LOD, are represented in Table 8. Linearity showed good correlation coefficient for all compounds ( $r^2 \geq 0.99$ ). These values showed to be suitable for monitoring of the target compounds in the urine samples of patients.

Table 8. Linearity parameters, LOQ and LOD for KYN, KA and TRP.

Analyte	Linearity			Limits	
	Range (ng/mL)	Linear Regression	Correlation coefficient ( $r^2$ )	LOD (ng/mL)	LOQ (ng/mL)
TRP	100 - 1100	$y = 0.03323x - 0.41248$	0.996	21.6	65.4
KYN	50 - 600	$y = 0.00099x - 0.0009$	0.993	13.1	39.8
KA	125 - 1500	$y = 0.00102x - 0.00726$	0.994	27.6	83.5

Accuracy and precision were evaluated using the three QC covering the linear range of the procedure. Accuracy was expressed as the closeness of agreement between the value determined by the method and the nominal concentration of the analyte, expressed in percentage. Precision was expressed as relative standard deviation percentage (% RSD). The three QCs were prepared and injected in triplicate. Table 9 summarizes the obtained values of accuracy and % RSD. The accuracy values obtained ranged from 98 to 111 showing that the method presents accuracy within acceptable values established by EMA (80 and 115%). Considering inter-day and intra-day precision % RSD varied between 2 and 15% which are in accordance with those demanded by EMA (under 15%), which means that the developed method is precise (Table 9).

Table 9. Accuracy, Intra-day and inter-day precision.

Analyte	Intra-day, inter-day precision and accuracy			
	Concentration (ng/mL)	Intra-day precision (%RSD)	Inter-day precision (%RSD)	Accuracy (%)
TRP	200	6.3	15.0	110
	550	3.5	3.4	110
	900	5.2	3.8	99
KYN	150	5.2	4.3	111
	300	5.3	4.8	111
	500	1.9	2.5	98
KA	375	4.0	6.4	108
	750	4.1	4.2	108
	1200	5.4	3.2	99

The three QCs concentrations used to precision and accuracy were also applied to recovery, each prepared in triplicate. Table 10 shows the recovery percentages for each analyte.

Table 10. Recovery

Analyte	Recovery (%)
TRP	106.5
	120.9
	95.2
KYN	117.5
	117.0
	102.6
KA	130.1
	119.7
	98.7

## 4.5. Method application

### 4.5.1 Urine samples from healthy individuals

A LC-UV-Vis/FD method was developed and validated for the simultaneous quantification TRP, KYN and KA in urine samples. Nevertheless, to investigate the adequacy of the method in terms of sensitivity (i.e. LOD and LOQ), accuracy, precision and linearity the method was applied to the quantification of the target compounds in urine samples from the healthy volunteers. Table 11 shows the urine concentrations of TRP, KYN and KA from healthy volunteers. Values ranged between 1139 and 3925 ng/mL for TRP, from < 40 to 724 ng/mL for KYN and from 846 ng/mL to 3329 ng/mL for KA.

Most studies regarding the development of chromatographic methods using urine samples did not perform the quantification of TRP and its metabolites in urine collected from healthy individuals. In fact, most applications are from spiked urine samples and not real samples. Further, Zhao *et al.* (2011) reported relative urinary values in healthy participants, i.e., concentrations were expressed as mmol metabolites/mol creatinine, rather than absolute urinary levels of TRP and its metabolites. Since the present study did not quantify neither serum or urinary creatinine levels from healthy volunteers, it is not possible to compare our absolute levels with data reported by Zhao *et al.* (2011). However, results obtained in healthy volunteers were used to compared with values of HF patients.



Table 11. Quantification of TRP, KYN and KA in the urine sample of healthy individuals.

Healthy individuals code	TRP, ng/mL	KYN, ng/mL	KA, ng/mL
2002	2942	<40	846
2003	3382	478	2517
2004	3925	224	1534
2007	1419	724	3329
2010	1139	699	2515

#### 4.5.2 Urine samples from HF patients

The method was further applied to the quantification of TRP and its metabolites in HF patients. Table 12 shows TRP and its metabolites concentrations in male patients (n = 18). Values ranged from 728 ng/mL to 8272 ng/mL for TRP, from 161 ng/mL to 997 ng/mL for KYN and 506 ng/mL to 2220 ng/mL for KA in the HF group. On the other hand, in the DM2/HF group the values varied between 1243 ng/mL and 4728 ng/mL for TRP, between 209 ng/mL and 908 ng/mL for KYN and 1105 ng/mL and 3433 ng/mL for KA.

The DM2/HF group showed higher values than those found for healthy volunteers, however, it was observed that the HF group showed lower values than those found for volunteers (Table 12).

The method was applied for quantification of the target compounds in the urine samples of both healthy volunteers and HF patients. In fact, a simple sample preparation procedure, low sample volume and a relative short analysis time satisfactory allowed the quantification of the analytes making the methodology useful to apply as a routine methodology for patient monitoring, as it is a fast method and uses a relatively inexpensive equipment (LC-UV-Vis/FD) and accessible to laboratories unlike other methods described in the bibliography. Other methods have been reported for the quantification of the TRP nevertheless, only few methods were reported considering the simultaneous quantification of TRP and its metabolites of the kynurenine pathway, implicated in heart disease in urine samples. For instance, Zhao *et al.* (2011), reported a LC-UV-FD method for the

simultaneous quantification of TRP and its metabolites and creatinine in urine samples. This methodology was only applied to health volunteers. Data was expressed in mmol/mol creatinine. LC-MS methods for the quantification of TRP, KYN and KA in urine samples have been reported (Lee *et al.* 2017; Oh *et al.* 2017). Nonetheless, this equipment is more expensive and is not found in many laboratories. On the other hand, most of the methods reported using LC-MS methods (Möller *et al.* 2012; Chen *et al.* 2018; Tong *et al.* 2018) used plasma as matrix.

There is also another study that used a GS-MS equipment to quantified metabolites of the kynurenine pathway in urine samples (Shin *et al.* 2017), however, optimization and validation was done in synthetic urine which makes validation simpler but does not take into account the possible interferences of the matrix.

**Table 12. Quantification of TRP and its metabolites in the urine sample of male patients in DM2/HF and HF groups and KYN/TRP and KA/KYN ratios.**

Analyte	HEALTHY GROUP (n = 5)	<i>p</i> value	HF (n=12)	DM2/HF (n =6)	<i>p</i> value
TRP, ng/mL	2942 [1280-3655]	<0.05	2875 [728-8272]	3127 [1243-4728]	0.89
KYN ng/mL	478 [<40-710]	<0.05	161 [161-997]	509 [209-908]	0.13
KA, ng/mL	2515 [1190-2925]	<0.05	1460 [506-2220]	1918 [1105-3433]	0.44
KYN/TRP ratio	0.3 [0.08-0.6]	0.09	0.1 [0.04-0.6]	0.3 [0.1-0.5]	0.73
KA/KYN ratio	5 [4-6]	<0.05	5 [2-14]	3 [2-5]	0.63

Values are expressed as median [Q1-Q3]

#### 4.6 Relationship between biochemical parameters, TRP and its metabolites.

Concentrations of the metabolites in the urine of the HF patients were used to calculate the KYN/TRP and KA/KYN ratios (Table 12), which indicate the activity of the IDO or TDO enzymes and KAT closely related to the activation of the immune system (Theofylaktopoulou *et al.* 2013; Birner *et al.* 2017). KYN/TRP ratio is usually increased in heart patients and is more evident in patients that have associated DM2 (Wirleitner *et al.* 2003). Corroborating with the literature, results showed a median of 0.3 KYN/TRP ratio for DM2/HF group while the HF group presented a lower value. Some metabolites of kynurenine pathway are known to have a neuroprotective role, namely KA (Pawlak *et al.* 2009). In addition, the KA/KYN ratio was pointed as a relevant neuroprotective marker of kynurenine pathway (Meier *et al.* 2018) and inflammatory situation being associated to a low production of KA compound (Pawlak *et al.* 2009). DM2/HF group presented lower KA/KYN ratio, compared with HF group, despite the higher median for KA compound of diabetic group. Moreover, both parameters were significantly lower compared with healthy group. Together, these results suggested that TRP metabolism proceeds along the kynurenine pathway through a different route in DM2/HF patients and possibly achieving distinct final products of the pathway. The increase of inflammatory state in diabetic patients (Chen *et al.* 2016) can be a plausible explanation for different results found between patient groups. Indeed, the biochemical data showed that DM2/HF patients had a mild increase in C-reactive protein levels compared with HF group, which are indicative of metabolic inflammatory state (Markanday 2015).

Body composition, particularly obesity is described as another condition that can have influence on the TRP metabolites ratios (Mangge *et al.* 2014). In fact, it was demonstrated that obese diabetic patients showed an elevation of KYN/TRP ratio (Rebnord *et al.* 2017). Data obtained in this study corroborate with these findings. For example, it was observed that 50% of the DM2/HF group were obese and presented a median KYN/TRP ratio of 0.4, while the remaining obese without DM2 patients a median of 0.06 (data not shown). Moreover, in opposite way, KA/KYN ratio was lower in obese of the DM2/HF group, about 4, while obese patients without DM2 showed a mean ratio of 16 (data not shown), these results raise to the

discussion of so-called “obesity paradox”, particularly the positive relation between obesity and neuroprotective (Clark *et al.* 2014).

Although obesity has been shown to be an independent risk factor for heart disease (Koliaki *et al.* 2019), over the past few years the hypothesis of “obesity paradox” in HF patients gained support (Clark *et al.* 2014), particularly in the case of an already developed disease. It has been shown that patients with BMI above 29.5 have more favorable prognosis and also heart disease indicators, such as BNP and more efficient kidney function (Clark *et al.* 2014). Moreover, decrease of BNP levels and higher eGFR were associated a more favorable hemodynamics of obese patients (Katsi *et al.* 2019). Regarding TRP metabolites ratios, it has been demonstrated that obese cardiac patients display a distinct ratio profile, lower KYN/TRP and higher KA/KYN ratios (Clark *et al.* 2014). This hypothesis is also observed in the present study.

It has been shown that BMI has an inverse relationship with the BNP concentration (Kinoshita *et al.* 2016; Katsi *et al.* 2019). However, the correlation between BMI and BNP was not evaluated in this study, but it was shown that both groups showed mean values above the normal reference value, which is common for heart patients (Cowley *et al.* 2004). The obese patients presented a mean of 154 pg/mL in contrast to the mean of 223 pg/mL in patients with BMI below 29.5 Kg/m<sup>2</sup>. For example, a particular case of a patient with underweight (BMI about 17 Kg/m<sup>2</sup>), which had a BNP plasma concentration of 286 pg/mL, while another case, one obese patient (BMI of 32 Kg/m<sup>2</sup>) presented a lower plasma BNP level (201 pg/mL) (data not shown).

High prevalence of hyponatremia in HF patients can have several causes (Mahmood *et al.* 2019). Among others, this is the most frequent cause is the decrease of blood volume in systemic circulation of HFrEF patients (Mahmood *et al.* 2019), which was diagnosed in all patients of this study. A recent study reported that the decrease of sodium levels in obese patients is not as marked as in patients with BMI < 29.5 (Davila and Udelson 2019). The present study failed to find similar results, difference that can be explained by the intensive use of diuretic therapy. In agreement with previous observations (Arévalo-Lorido *et al.* 2019), our results showed that 90% of

all male HF patients consume one or more diuretic drugs (data not shown), which is associated with low concentration of  $\text{Na}^+$ , suggestive of diuretic-induced hyponatremia. On the other hand, it is known that hyperuricemia can provoke the release of pro-inflammatory cytokine and also is considered as a marker for oxidative metabolism (Shirakabe *et al.* 2019). The research reported here corroborates these observations and provides additional evidence for the kynurenine pathway as a possible mechanism underlying the pathophysiology of HF patients. Biochemical data herein showed that 53% ( $n = 10$ ) of male patients showed uric acid levels above normal reference values, more than 40% ( $n = 4$ ) showed higher levels of C-reactive protein. Moreover, the TRP metabolism results showed that 40% ( $n = 4$ ) of these patients present a decrease of TRP concentration associated with a decrease of KA compound (data not shown), corroborating the link between pro-oxidative environment and deregulation of kynurenine pathway (Wang *et al.* 2015). For example, in the case of one particular DM2/HF patient, biochemical data indicated the presence of hyperuricemia (with uric acid levels of 9.3 mg/dL) and C-reactive protein levels of 8 mg/L. In addition, this patient showed a KYN/TRP ratio above the median for his group, while presented the lowest KA/KYN ratio (data not shown), supporting the positive association between hyperuricemia and inflammation, which could interfere with TRP metabolism.

Another important biochemical parameter to describe is serum HDL-c concentrations in HF patients, since this lipoprotein has positive effects on apoptosis, attenuates oxidative stress and promotes the reabsorption of glucose by cardiomyocytes (Gomaschi *et al.* 2016; Potočnjak *et al.* 2017). HDL-c still plays a key role in regulating the release of pro-inflammatory cytokines and ROS production, moreover, the ability of HDL-c to regulate  $\text{TNF}\alpha$  is particularly relevant in cardiomyocytes (Gomaschi *et al.* 2016). Previous research reported an alteration of inflammation markers in patients with very low HDL-c levels (from 10 mg/dL to 29 mg/dL) (Roe *et al.* 2008). In this study, 79% ( $n = 15$ ) of HF patients showed the lower levels for HDL-c (less than 29 mg/dL) and mean concentration of  $\sim 3$  mg/L for C-reactive protein. The other 21% of the patients showed a higher mean for HDL-c (33 mg/dL) and a lower mean concentration of C-reactive protein ( $\sim 1$

mg/L). Moreover, in one particular case, a DM2/HF patient showed the lowest value of HDL-c (8.7 mg/dL) and the higher concentration of C-reactive protein (8 mg/L). In this case, the KYN/TRP ratio was above the median of his group (0.3), meanwhile KA/KYN ratio was of  $\sim 1.7$ , the lowest value of the group (data not shown). All together, these results gives support to the hypothesis that KYN/TRP ratio is related with IDO activity and KA/KYN ratio can be a good neuroprotector indicator, probably more relevant than KA metabolite alone (Theofylaktopoulou *et al.* 2013; Birner *et al.* 2017).

.

## 6. CONCLUSION

This work presents the development and validation of a method suitable for the simultaneous quantification of TRP and metabolites involved in the kynurenine pathway in urine samples from healthy volunteers and HF patients. The present method uses a simple sample preparation procedure, low sample volume and a satisfactory identification and quantification of TRP and its metabolites in urine samples. In fact, most methods use other matrices such as plasma or serum. Urine matrices offers the important advantage of simplicity in sample collection, i.e., do not require invasive procedures. From the clinical point of view, the quantification of TRP and its metabolites allowed the determination of the KYN/TRP and KA/KYN ratios which can provide important insights about the diagnose and prognostic of HF patients.

This study was able to demonstrate the negative influence of comorbid diabetes in patients with chronic heart failure, particularly on kidney function, inflammatory status and kynurenine pathway of TRP metabolism. It was able to corroborate the link between HF, inflammation and kynurenergic pathway by comparing TRP metabolites and biochemical markers (related with cardiac function or inflammatory status) such as BNP, CK, HDL-c, C-reactive protein and uric acid. Our findings confirm the existence of "obesity paradox" in patients with already-established HF<sub>rEF</sub>, by providing evidence to support an inverse relationship between BMI and BNP. This study provides additional information about the link between comorbid obesity and kynurenine pathway metabolites, showing a distinct TRP metabolites profile of these patients and, TRP metabolism proceed via KA formation, which is known to have neuroprotective effects.

In summary, this study allowed to conclude the high relevance of this metabolic pathway in HF patients with or without comorbidities and its links with other unbalanced states of the organism and, therefore, the development of methods capable of quantifying these metabolites in a simple and efficient way with the least possible sacrifice of the patients during the collection of the samples is of great importance.

## **6.1 Limitations**

This work, due to the character of a pilot project, welcomed a small number of patients under study, which eventually limited the possible conclusions to be drawn. The impossibility of using a mass equipment to arrive at a more precise identification of the analytes. It was also not possible to quantify some enzymes of the kynurenine pathway due to the complexity of the necessary reagents.

Finally, it was not possible to validate the method for the second biological matrix, plasma, as initially proposed due to global contingency.

## **6.2 Future perspectives**

Considering the favorable results obtained for this matrix (urine) it is relevant to proceed with the validation of a method capable of identifying and quantifying the same analytes but in plasma, so that a relationship between the concentration of these analytes in urine and plasma can then be found.

It will also be important to extend it to more patients so that stronger and more sustained conclusions can be drawn. In addition to include more parameters to be analyzed such as the quantification of some specific cardiac function enzymes and enzymes involved in the Kynurenine pathway.

In order to implement the analysis of these analytes in urine and thus allow a less invasive sample collection.



## 7. BIBLIOGRAPHY

Arévalo-Lorido JC, Carretero-Gómez J, Robles NR, et al. Prognostic Role of Hyponatremia in Heart Failure Patients Depending on Renal Disease: Clinical Evidence. *Cardiology* 144(1–2): 1–8, 2019.

Arimon M, Takeda S, Post KL, et al. Oxidative Stress and Lipid Peroxidation Are Upstream of Amyloid Pathology. *Neurobiology of Disease* 84: 109–119, 2015.

Assem M, Lando M, Grissi M, et al. The Impact of Uremic Toxins on Cerebrovascular and Cognitive Disorders. *Toxins* 10(7): 303, 2018.

Ayoub KF, Pothineni NVK, Rutland J, Ding Z, Mehta JL. Immunity, Inflammation, and Oxidative Stress in Heart Failure: Emerging Molecular Targets. *Cardiovascular Drugs and Therapy* 31(5–6): 593–608, 2017.

Badawy A. Kynurenine Pathway of Tryptophan Metabolism: Regulatory and Functional Aspects. *International Journal of Tryptophan Research* 10: 117864691769193, 2017.

Badawy A. Kynurenine Pathway and Human Systems. *Experimental Gerontology* 129: 110770, 2020.

Benjamin EJ, Blaha MJ, Chiuve SE, et al. Heart Disease and Stroke Statistics-2017 Update: A Report From the American Heart Association. *Circulation* 135(10): e146–e603, 2017.

Birner A, Platzer M, Bengesser SA, et al. Increased Breakdown of Kynurenine towards Its Neurotoxic Branch in Bipolar Disorder. *PLoS One* 12(2): e0172699, 2017.

Black S, Kushner I, Samols D. C-Reactive Protein. *Journal of Biological Chemistry* 279(47): 48487–48490, 2004.

Braunwald E. Biomarkers in Heart Failure. *The New England Journal of Medicine* 358(20): 2148–2159, 2008.

Bui AL, Horwich TB, Fonarow GC. Epidemiology and Risk Profile of Heart Failure. *Nature Reviews. Cardiology* 8(1): 30–41, 2011.

Cao Z, Jia Y, Zhu B. BNP and NT-ProBNP as Diagnostic Biomarkers for Cardiac Dysfunction in Both Clinical and Forensic Medicine. *International Journal of Molecular Sciences* 20(8): 1820, 2019.

Çelik SF, Karakurt C, Tabel Y, Elmas T, Yoloğlu S. Blood Pressure Is Normal, but Is the Heart? *Pediatric Nephrology* 33(9): 1585–1591, 2018.

Cervenka I, Agudelo LZ, Ruas JL. Kynurenines: Tryptophan's Metabolites in Exercise, Inflammation, and Mental Health. *Science* 357(6349): eaaf9794, 2017.

Chen Y, Chen H, Shi G, et al. Ultra-Performance Liquid Chromatography-Tandem Mass Spectrometry Quantitative Profiling of Tryptophan Metabolites in Human Plasma and Its Application to Clinical Study. *Journal of Chromatography B*, 2019.

Chen Q, Zhang Y, Ding D, et al. Associations between Serum Calcium, Phosphorus and Mortality among Patients with Coronary Heart Disease. *European Journal of Nutrition* 57(7): 2457–2467, 2018.

Chen T, Zheng X, Ma X, et al. Tryptophan Predicts the Risk for Future Type 2 Diabetes. *PLOS ONE* 11(9), 2016.

Clark AL, Fonarow GC, Horwich TB. Obesity and the Obesity Paradox in Heart Failure. *Progress in Cardiovascular Diseases* 56(4): 409–414, 2014.

Connor TJ, Starr N, O'Sullivan JB, Harkin A. Induction of Indolamine 2,3-Dioxygenase and Kynurenine 3-Monooxygenase in Rat Brain Following a Systemic Inflammatory Challenge: A Role for IFN-Gamma? *Neuroscience Letters* 441(1): 29–34, 2008.

Costa S, Reina-Couto M, Albino-Teixeira A, Sousa T. Estatinas e stresse oxidativo na insuficiência cardíaca crónica. *Revista Portuguesa de Cardiologia* 35(1): 41–57, 2016.

Cowley CG, Bradley JD, Shaddy RE. B-Type Natriuretic Peptide Levels in Congenital Heart Disease. *Pediatric Cardiology* 25(4), 2004.

Damman K, Testani JM. The Kidney in Heart Failure: An Update. *European Heart Journal* 36(23): 1437–1444, 2015.

Davila CD, Udelson JE. Hypervolemic Hyponatremia in Heart Failure. *In* *Frontiers of Hormone Research*. Alessandro Peri, Chris J. Thompson, and Joseph G. Verbalis, eds. Pp. 113–129. S. Karger AG, 2019.

de Almeida ML, Saatkamp CJ, Fernandes AB, Barbosa AL Pinheiro, Silveira L. Estimating the Concentration of Urea and Creatinine in the Human Serum of Normal and Dialysis Patients through Raman Spectroscopy. *Lasers in Medical Science* 31(7): 1415–1423, 2016.

Dimova ED, Mohan ARM, Swanson V, Evans JMM. Interventions for Prevention of Type 2 Diabetes in Relatives: A Systematic Review. *Primary Care Diabetes* 11(4): 313–326, 2017.

Dröge W. Free Radicals in the Physiological Control of Cell Function. *Physiological Reviews* 82(1): 47–95, 2002.

Fetoni AR, Paciello F, Rolesi R, Paludetti G, Troiani D. Targeting Dysregulation of Redox Homeostasis in Noise-Induced Hearing Loss: Oxidative Stress and ROS Signaling. *Free Radical Biology and Medicine* 135: 46–59, 2019.

Flegal KM, Kit BK, Orpana H, Graubard BI. Association of All-Cause Mortality With Overweight and Obesity Using Standard Body Mass Index Categories: 12, 2013.

Fowler ED, Benoist D, Drinkhill MJ, et al. Decreased Creatine Kinase Is Linked to Diastolic Dysfunction in Rats with Right Heart Failure Induced by Pulmonary Artery Hypertension. *Journal of Molecular and Cellular Cardiology* 86: 1–8, 2015.

Fu D. Cardiac Arrhythmias: Diagnosis, Symptoms, and Treatments. *Cell Biochemistry and Biophysics* 73(2): 291–296, 2015.

Gobaille S, Kemmel V, Brumar D, et al. Xanthurenic Acid Distribution, Transport, Accumulation and Release in the Rat Brain. *Journal of Neurochemistry* 105(3): 982–993, 2008.

Goicoechea M, Vinuesa SG, Verdalles U, et al. Effect of Allopurinol in Chronic Kidney Disease Progression and Cardiovascular Risk. *Clinical Journal of the American Society of Nephrology* 5(8): 1388–1393, 2010.

Gölbapý Z, Uçar Ö, Yüksel AG, et al. Plasma Brain Natriuretic Peptide Levels in Patients with Rheumatic Heart Disease. *European Journal of Heart Failure* 6(6): 757–760, 2004.

Gomaschi M, Calabresi L, Franceschini G. Protective Effects of HDL Against Ischemia/Reperfusion Injury. *Frontiers in Pharmacology* 7, 2016.

González E, Ramírez-Ortega D, Pineda B, et al. Kynurenine Pathway Metabolites and Enzymes Involved in Redox Reactions. *Neuropharmacology* 112: 331–345, 2017.

Greenberg B. Managing Hyponatremia in Patients with Heart Failure. *Journal of Hospital Medicine* 5(S3): S33–S39, 2010.

Grodin JL, Testani JM, Pandey A, et al. Perturbations in Serum Chloride Homeostasis in Heart Failure with Preserved Ejection Fraction: Insights from TOPCAT: Serum Chloride in HFpEF. *European Journal of Heart Failure* 20(10): 1436–1443, 2018.

Guideline-Bioanalytical-Method-Validation\_EMA, 2011.

Hasanzad M, Sarhangi N, Meybodi HRA, et al. Precision Medicine in Non Communicable Diseases. *International Journal of Molecular and Cellular Medicine* 8(Suppl1): 1–18, 2019.

Heine W, Radke M, Wutzke KD. The Significance of Tryptophan in Human Nutrition. *Amino Acids* 9(3): 91–205, 1995.

Hu J, Xi D, Zhao J, et al. High-Density Lipoprotein and Inflammation and Its Significance to Atherosclerosis. *The American Journal of the Medical Sciences* 352(4): 408–415, 2016.

Hu LJ, Li XF, Hu JQ, et al. A Simple HPLC-MS/MS Method for Determination of Tryptophan, Kynurenine and Kynurenic Acid in Human Serum and Its Potential for Monitoring Antidepressant Therapy. *Journal of Analytical Toxicology* 41(1): 37–44, 2017.

Hunt SA, Baker DW, Chin MH, et al. ACC/AHA Guidelines for the Evaluation and Management of Chronic Heart Failure in the Adult: Executive Summary A Report of the American College of Cardiology/American Heart Association Task Force on Practice Guidelines (Committee to Revise the 1995 Guidelines for the Evaluation and Management of Heart Failure): Developed in Collaboration With the International Society for Heart and Lung Transplantation; Endorsed by the Heart Failure Society of America. *Circulation* 104(24): 2996–3007, 2001.

Karam BS, Chavez-Moreno A, Koh W, Akar JG, Akar FG. Oxidative Stress and Inflammation as Central Mediators of Atrial Fibrillation in Obesity and Diabetes. *Cardiovascular Diabetology* 16(1): 120, 2017.

Karu N, McKercher C, Nichols DS, et al. Tryptophan Metabolism, Its Relation to Inflammation and Stress Markers and Association with Psychological and Cognitive Functioning: Tasmanian Chronic Kidney Disease Pilot Study. *BMC Nephrology* 17, 2016.

Kato J, Kawagoe Y, Jiang D, et al. Plasma Levels of Natriuretic Peptides and Year-by-Year Blood Pressure Variability: A Population-Based Study. *Journal of Human Hypertension* 31(8): 525–529, 2017.

Katsi V, Marketou M, Antonopoulos AS, et al. B-Type Natriuretic Peptide Levels and Benign Adiposity in Obese Heart Failure Patients. *Heart Failure Reviews* 24(2): 219–226, 2019.

Kattoor AJ, Pothineni NVK, Palagiri D, Mehta JL. Oxidative Stress in Atherosclerosis. *Current Atherosclerosis Reports* 19(11): 42, 2017.

Koji K, Kawai M, Minai K, et al. Potent Influence of Obesity on Suppression of Plasma B-Type Natriuretic Peptide Levels in Patients with Acute Heart Failure: An Approach Using Covariance Structure Analysis. *International Journal of Cardiology* 215: 283–290, 2016.

Koliaki C, Liatis S, Kokkinos A. Obesity and Cardiovascular Disease: Revisiting an Old Relationship. *Metabolism* 92: 98–107, 2019.

Kopin L, Lowenstein CJ. Dyslipidemia. *Annals of Internal Medicine* 167(11): ITC81, 2017.

Krcmova L, Solichova D, Melichar B, et al. Determination of Neopterin, Kynurenine, Tryptophan and Creatinine in Human Serum by High Throuput HPLC. *Talanta* 85(3): 1466–1471, 2011.

Kunutsor SK, Zaccardi F, Karppi J, Kurl S, Laukkanen JA. Is High Serum LDL/HDL Cholesterol Ratio an Emerging Risk Factor for Sudden Cardiac Death? Findings from the KIID Study. *Journal of Atherosclerosis and Thrombosis* 24(6): 600–608, 2017.

Laecke SV. Hypomagnesemia and hypermagnesemia, *Acta Clinica Belgica*, 74:1, 41-47, 2019.

Lau WL, Vaziri ND. Urea, a True Uremic Toxin: The Empire Strikes Back. *Clinical Science* 131(1): 3–12, 2017.

Lee W, Park NH, Ahn TB, Chung BC, Hong J. Profiling of a Wide Range of Neurochemicals in Human Urine by Very-High-Performance Liquid Chromatography-Tandem Mass Spectrometry Combined with in Situ Selective Derivatization. *Journal of Chromatography A* 1526: 47–57, 2017.

Lehrke M, Marx N. Diabetes Mellitus and Heart Failure. *The American Journal of Cardiology* 120(1): S37–S47, 2017.

Lepojärvi ES, Huikuri HV, Piira OP, et al. Biomarkers as Predictors of Sudden Cardiac Death in Coronary Artery Disease Patients with Preserved Left Ventricular Function (ARTEMIS Study). *PLoS One* 13(9): e0203363, 2018.

Li YR, Trush M. Defining ROS in Biology and Medicine. *Reactive Oxygen Species* 1(1), 2016.

Linthou SV, Tschöpe C. Inflammation - Cause or Consequence of Heart Failure or Both? *Current Heart Failure Reports* 14(4): 251–265, 2017.

Liu J-J, Movassat J and Portha B. «Emerging Role for Kynurenines in Metabolic Pathologies». *Current Opinion in Clinical Nutrition & Metabolic Care* 22(1): 82–90, 2019.

Mahmood T, Raj K, Ehtesham M, et al. Serum Sodium Profile of Congestive Heart Failure Patients and Its Impact on Their Outcome at Discharge. *Cureus Journal of Medical Science* 11(8), 2019.

Mangge H, Summers KL, Meinitzer A, et al. Obesity-Related Dysregulation of the Tryptophan-Kynurenine Metabolism: Role of Age and Parameters of the Metabolic Syndrome: Tryptophan Metabolism and Inflammation in Obesity. *Obesity* 22(1): 195–201, 2014.

Markanday A. Acute Phase Reactants in Infections: Evidence-Based Review and a Guide for Clinicians. *Open Forum Infectious Diseases*, Volume 2, Issue 3, Summer 2015, ofv098

Mathers C, Stevens G, Hogan D, Mahanani WR, Ho J. Global and Regional Causes of Death: Patterns and Trends, 2000–15. *In* Disease Control Priorities: Improving Health and Reducing Poverty. 3rd edition. Dean T. Jamison, Hellen Gelband, Susan

Horton, et al., eds. Washington (DC): The International Bank for Reconstruction and Development / The World Bank, 2017.

May HT, Horne BD, Knight S, et al. The Association of Depression at Any Time to the Risk of Death Following Coronary Artery Disease Diagnosis. *European Heart Journal. Quality of Care & Clinical Outcomes* 3(4): 296–302, 2017.

McCormack T, Dent R, Blagden M. Very Low LDL-C Levels May Safely Provide Additional Clinical Cardiovascular Benefit: The Evidence to Date. *International Journal of Clinical Practice* 70(11): 886–897, 2016.

McLeish MJ, Kenyon GL. Relating Structure to Mechanism in Creatine Kinase. *Critical Reviews in Biochemistry and Molecular Biology* 40(1): 1–20, 2005.

Meier TB, Drevets WC, Teague TK, et al. Kynurenic Acid Is Reduced in Females and Oral Contraceptive Users: Implications for Depression. *Brain, Behavior, and Immunity* 67: 59–64, 2018.

de Mello AH, Costa AB, Engel JDG, Rezin GT. Mitochondrial Dysfunction in Obesity. *Life Sciences* 192: 26–32, 2018.

Moffett JR, Namboodiri MA. Tryptophan and the Immune Response. *Immunology and Cell Biology* 81(4): 247–265, 2003.

Möller M, Preez JLD, Harvey BH. Development and Validation of a Single Analytical Method for the Determination of Tryptophan, and Its Kynurenine Metabolites in Rat Plasma. *Journal of Chromatography B* 898: 121–129, 2012.

Mosterd A, Hoes AW. Clinical Epidemiology of Heart Failure. *Heart (British Cardiac Society)* 93(9): 1137–1146, 2007.

Ndrepepa G. Uric Acid and Cardiovascular Disease. *Clinica Chimica Acta* 484: 150–163, 2018.

NHFA CSANZ Heart Failure Guidelines Working Group, John J. Atherton, Andrew Sindone, et al. National Heart Foundation of Australia and Cardiac Society of Australia and New Zealand: Guidelines for the Prevention, Detection, and Management of Heart Failure in Australia 2018. *Heart, Lung & Circulation* 27(10): 1123–1208, 2018.

Nichols M, Townsend N, Scarborough P, Rayner M. Cardiovascular Disease in Europe 2014: Epidemiological Update. *European Heart Journal* 35(42): 2929, 2014.

Nicklas BJ, Cesari M, Penninx BWJH, et al. Abdominal Obesity Is an Independent Risk Factor for Chronic Heart Failure in Older People: ABDOMINAL OBESITY AND HEART FAILURE. *Journal of the American Geriatrics Society* 54(3): 413–420, 2006.

Niki E. Lipid Peroxidation Products as Oxidative Stress Biomarkers. *BioFactors* 34(2): 171–180, 2008.

Nikkheslat N, Zunszain PA, Horowitz MA, et al. Insufficient Glucocorticoid Signaling and Elevated Inflammation in Coronary Heart Disease Patients with Comorbid Depression. *Brain, Behavior, and Immunity* 48: 8–18, 2015.

Oh JS, Seo HS, Kim KH, et al. Urinary Profiling of Tryptophan and Its Related Metabolites in Patients with Metabolic Syndrome by Liquid Chromatography-Electrospray Ionization/Mass Spectrometry. *Analytical and Bioanalytical Chemistry* 409(23): 5501–5512, 2017.

Ortiz GI, Fariña-López RM, Rodríguez SAI, Achinelli CEC. Presión Arterial Elevada y Otros Factores de Riesgo Cardiovascular En Estudiantes de La Universidad Nacional de Asunción-Paraguay. *Revista de La Facultad de Ciencias Médicas de Córdoba* 76(2): 79, 2019.

Palazzuoli A, Ruocco G, Vivo O, Nuti R, McCullough PA. Prevalence of Hyperuricemia in Patients With Acute Heart Failure With Either Reduced or Preserved Ejection Fraction. *The American Journal of Cardiology* 120(7): 1146–1150, 2017.

Pawlak K, Brzosko S, Mysliwiec M, Pawlak D. Kynurenine, Quinolinic Acid—The New Factors Linked to Carotid Atherosclerosis in Patients with End-Stage Renal Disease. *Atherosclerosis* 204(2): 561–566, 2009.

Peoples JN, Saraf A, Ghazal N, Pham TT, Kwong JQ. Mitochondrial Dysfunction and Oxidative Stress in Heart Disease. *Experimental & Molecular Medicine* 51(12): 1–13, 2019.

Pertovaara M, Raitala A, Juonala M, et al. Indoleamine 2,3-Dioxygenase Enzyme Activity Correlates with Risk Factors for Atherosclerosis: The Cardiovascular Risk in Young Finns Study. *Clinical and Experimental Immunology* 148(1): 106–111, 2007.

Piano MR, Phillips SA. Alcoholic Cardiomyopathy: Pathophysiologic Insights. *Cardiovascular Toxicology* 14(4): 291–308, 2014.



Pinhati RR, Polonini HC, Brandão MAF, et al. Quantification of Tryptophan in Plasma by High Performance Liquid Chromatography. *Química Nova* 35(3): 623–626, 2012.

Polyzos KA, Ketelhuth DFJ. The Role of the Kynurenine Pathway of Tryptophan Metabolism in Cardiovascular Disease. An Emerging Field. *Hamostaseologie* 35(2): 128–136, 2015.

Potočnjak I, Degoricija V, Trbušić M, et al. Serum Concentration of HDL Particles Predicts Mortality in Acute Heart Failure Patients. *Scientific Reports* 7(1): 46642, 2017.

Rebnord EW, Strand E, Midttun O, et al. The Kynurenine:Tryptophan Ratio as a Predictor of Incident Type 2 Diabetes Mellitus in Individuals with Coronary Artery Disease. *Diabetologia* 60(9): 1712–1721, 2017

Rehman K, Akash MSH. Mechanism of Generation of Oxidative Stress and Pathophysiology of Type 2 Diabetes Mellitus: How Are They Interlinked?: OXIDATIVE STRESS AND DIABETES MELLITUS. *Journal of Cellular Biochemistry* 118(11): 3577–3585, 2017.

Reyes AJ. Cardiovascular Drugs and Serum Uric Acid. *Cardiovascular Drugs and Therapy* 17(5/6): 397–414, 2003.

Rhoads JP, Major AS. How Oxidized Low-Density Lipoprotein Activates Inflammatory Responses. *Critical Reviews in Immunology* 38(4): 333–342, 2018.

Rocca HPBL, Wijk SV. Natriuretic Peptides in Chronic Heart Failure. *Card Fail Rev.* 2019 Feb;5(1):44-49, 2019.

Roe MT, Ou FS, Alexander KP, et al. Patterns and Prognostic Implications of Low High-Density Lipoprotein Levels in Patients with Non-ST-Segment Elevation Acute Coronary Syndromes. *European Heart Journal* 29(20): 2480–2488, 2008.

Rutledge T, Reis VA, Linke SE, Greenberg BH, Mills PJ. Depression in Heart Failure a Meta-Analytic Review of Prevalence, Intervention Effects, and Associations with Clinical Outcomes. *Journal of the American College of Cardiology* 48(8): 1527–1537, 2006.

Sadok I, Gamian A, Staniszewska MM. Chromatographic Analysis of Tryptophan Metabolites. *Journal of Separation Science* 40(15): 3020–3045, 2017.

Shin HJ, Park NH, Lee W, et al. Metabolic Profiling of Tyrosine, Tryptophan, and Glutamate in Human Urine Using Gas Chromatography–Tandem Mass Spectrometry Combined with Single SPE Cleanup. *Journal of Chromatography B* 1051: 97–107, 2017.

Shirakabe A, Okazaki H, Matsushita M, et al. Hyperuricemia Complicated with Acute Kidney Injury Is Associated with Adverse Outcomes in Patients with Severely Decompensated Acute Heart Failure. *IJC Heart & Vasculature* 23: 100345, 2019.

Shirazi LF, Bissett J, Romeo F, Mehta JL. Role of Inflammation in Heart Failure. *Current Atherosclerosis Reports* 19(6): 27, 2017.

Shrimanker I, Bhattarai S. *Electrolytes. In StatPearls*. Treasure Island (FL): StatPearls Publishing, 2020.

Song P, Ramprasath T, Wang H, Zou MH. Abnormal Kynurenine Pathway of Tryptophan Catabolism in Cardiovascular Diseases. *Cellular and Molecular Life Sciences: CMLS* 74(16): 2899–2916, 2017.

Sorgdrager FJH, Naudé PJW, Kema IP, Nollen KA, De Deyn PP. Tryptophan Metabolism in Inflammaging: From Biomarker to Therapeutic Target. *Frontiers in Immunology* 10: 2565, 2019.

de Souza JA, Vindis C, Nègre-Salvayre A, et al. Small, Dense HDL3 Particles Attenuates Apoptosis in Endothelial Cells: Pivotal Role of Apolipoprotein A-I. *Journal of Cellular and Molecular Medicine*, 2009.

Stone TW. Kynurenic Acid Antagonists and Kynurenine Pathway Inhibitors. *Expert Opinion on Investigational Drugs* 10(4): 633–645, 2001.

Sun XD, Wu HL, Liu Z, et al. Target-Based Metabolomics for Fast and Sensitive Quantification of Eight Small Molecules in Human Urine Using HPLC-DAD and Chemometrics Tools Resolving of Highly Overlapping Peaks. *Talanta* 201: 174–184, 2019.

Thackray SJ, Mowat CG, Chapman SK. Exploring the Mechanism of Tryptophan 2,3-Dioxygenase. *Biochemical Society Transactions* 36(6): 1120–1123, 2008.

Theofylaktopoulou D, Midttun, Ulvik A, et al. A Community-Based Study on Determinants of Circulating Markers of Cellular Immune Activation and Kynurenines:

The Hordaland Health Study. *Clinical and Experimental Immunology* 173(1): 121–130, 2013.

Thevandavakkam MA, Schwarcz R, Muchowski PJ, Giorgini G. Targeting Kynurenine 3-Monooxygenase (KMO): Implications for Therapy in Huntington's Disease. *CNS & Neurological Disorders Drug Targets* 9(6): 791–800, 2010.

Timmis A, Townsend N, Gale CP, et al. European Society of Cardiology: Cardiovascular Disease Statistics 2019. *European Heart Journal* 41(1): 12–85, 2020.

Tong Q, Song J, Yang G, et al. Simultaneous Determination of Tryptophan, Kynurenine, Kynurenic Acid, Xanthurenic Acid and 5-Hydroxytryptamine in Human Plasma by LC-MS/MS and Its Application to Acute Myocardial Infarction Monitoring. *Biomedical Chromatography* 32(4): e4156, 2018.

Tuba M, Ehtesham RKM, et al. Serum Sodium Profile of Congestive Heart Failure Patients and Its Impact on Their Outcome at Discharge. *Cureus* 11(8), 2019.

de la Torre JC. Is Alzheimer's Disease a Neurodegenerative or a Vascular Disorder? Data, Dogma, and Dialectics. *The Lancet. Neurology* 3(3): 184–190, 2004.

Valko M, Leibfritz D, Moncol J, et al. Free Radicals and Antioxidants in Normal Physiological Functions and Human Disease. *The International Journal of Biochemistry & Cell Biology* 39(1): 44–84, 2007.

Laecke SV. Hypomagnesemia and Hypermagnesemia. *Acta Clinica Belgica* 74(1): 41–47, 2019.

Vedin O, Lam CSP, Koh AS, et al. Significance of Ischemic Heart Disease in Patients With Heart Failure and Preserved, Midrange, and Reduced Ejection Fraction: A Nationwide Cohort Study. *Circulation. Heart Failure* 10(6), 2017.

Vignau J, Lefort MCJA, Imbenotte M, Lhermitte M. Simultaneous Determination of Tryptophan and Kynurenine in Serum by HPLC with UV and Fluorescence Detection. *Biomedical Chromatography* 18(10): 872–874, 2004.

Wagner CJ, Musenbichler C, Böhm L, et al. LDL Cholesterol Relates to Depression, Its Severity, and the Prospective Course. *Progress in Neuro-Psychopharmacology and Biological Psychiatry* 92: 405–411, 2019.

Wang Q, Liu D, Song P, Zou MH. Tryptophan-Kynurenine Pathway Is Dysregulated in

Inflammation, and Immune Activation. *Frontiers in Bioscience (Landmark Edition)* 20: 1116–1143, 2015.

Want EJ. LC-MS Untargeted Analysis. *In* *Metabolic Profiling*. Georgios A. Theodoridis, Helen G. Gika, and Ian D. Wilson, eds. Pp. 99–116. *Methods in Molecular Biology*. New York, NY: Springer New York, 2018.

Wigner P, Czarny P, Galecki P, Su KP, Sliwinski T. The Molecular Aspects of Oxidative & Nitrosative Stress and the Tryptophan Catabolites Pathway (TRYCATs) as Potential Causes of Depression. *Psychiatry Research* 262: 566–574, 2018.

Wirleitner B, Rudzite V, Neurauder G, et al. Immune Activation and Degradation of Tryptophan in Coronary Heart Disease. *European Journal of Clinical Investigation* 33(7): 550–554, 2003.

Wu AH, Gladden JD, Ahmed M, Ahmed A, Filippatos G. Relation of Serum Uric Acid to Cardiovascular Disease. *International Journal of Cardiology* 213: 4–7, 2016.

Zagajewski J, Drozdowicz D, Brzozowska I, et al. Conversion l-tryptophan to melatonin in the gastrointestinal tract: the new high performance liquid chromatography method enabling simultaneous determination of six metabolites of l-tryptophan by native fluorescence and uv-vis detection: 9, 2012.

Zhao J, Chen H, Ni P, et al. Simultaneous Determination of Urinary Tryptophan, Tryptophan-Related Metabolites and Creatinine by High Performance Liquid Chromatography with Ultraviolet and Fluorimetric Detection. *Journal of Chromatography B* 879(26): 2720–2725, 2011.

Zhu W, Stevens AP, Dettmer K, et al. Quantitative Profiling of Tryptophan Metabolites in Serum, Urine, and Cell Culture Supernatants by Liquid Chromatography–Tandem Mass Spectrometry. *Analytical and Bioanalytical Chemistry* 401(10): 3249–3261, 2011.

Ziaeeian B, Fonarow GC. Epidemiology and Aetiology of Heart Failure. *Nature Reviews. Cardiology* 13(6): 368–378, 2016.

Zou MH. Tryptophan-Kynurenine Pathway Is Dysregulated in Inflammation and Immune Activation. *Frontiers in Bioscience* 20(7): 1116–1143, 2015.

Zuo H, Ueland PM, Ulvik A, et al. Plasma Biomarkers of Inflammation, the Kynurenine Pathway, and Risks of All-Cause, Cancer, and Cardiovascular Disease

Mortality: The Hordaland Health Study. *American Journal of Epidemiology* 183(4): 249–258, 2016.

## 8. ANNEXES

**Annex I** - Table 1S: Sample preparations tested throughout the method development process

**Annex II** - Abstract and poster of the "3ª Reunião internacional da RACS"

## Annex I.

Table 1S: Sample preparations tested throughout the method development process

Procedure	solvent	pH	DF	centrifugation	Filter (Pore size)	V evaporated ( $\mu$ L)	V reconstituted ( $\mu$ L)
1	UPW with 0.01% TFA	3	10X	15min; 13000 r.p.m at 4 °C			
2	UPW with 0.01% TFA	3	10X	15min; 13000 r.p.m at 4 °C			
3	UPW with 0.01% TFA	3	5x	15min; 13000 r.p.m at 4 °C			
4	UPW with 0.01% TFA	3	5x	15min; 13000 r.p.m at 4 °C			
5	UPW with 0.01% TFA	3	10x	2x 15min; 13000 r.p.m at 4 °C			
6	UPW with 0.01% TFA	3	10x	2x 15min; 13000 r.p.m at 4 °C			
7	UPW with 0.01% TFA	3	5x	2x 15min; 13000 r.p.m at 4 °C			
8	UPW with 0.01% TFA	3	5x	2x 15min; 13000 r.p.m at 4 °C			
9	20 mM ammonium formate in UPW with 0.01% formic acid	4.4	10x	2x 15min; 13000 r.p.m at 4 °C	22 $\mu$ m		
10	20 mM ammonium formate in ultrapure water with 0.01% formic acid	4.4	10x	2x 15min; 13000 r.p.m at 4 °C	22 $\mu$ m		
11	20 mM ammonium formate in ultrapure water with 0.01% formic acid	4.4	5x	2x 15min; 13000 r.p.m at 4 °C	22 $\mu$ m		

12	20 mM ammonium formate in ultrapure water with 0.01% formic acid	4,4	5x	2x 15min;13000 r.p.m at 4 °C	22 µm		
13	20 mM ammonium formate in ultrapure water with 0.01% formic acid	4,4	5x	2x 15min;13000 r.p.m at 4 °C	22 µm		
14	20 mM ammonium formate in ultrapure water with 0.01% formic acid	4,4	5x	2x 15min;13000 r.p.m at 4 °C	22 µm		
15	20 mM ammonium formate in ultrapure water with 0.01% formic acid	4,4	2x	2x 15min;13000 r.p.m at 4 °C	22 µm		
16	20 mM ammonium formate in ultrapure water with 0.01% formic acid	4,4	2x	2x 15min;13000 r.p.m at 4 °C	22 µm		
17	20 mM ammonium formate in ultrapure water with 0.01% formic acid	4,4	1.1	2x 15min;13000 r.p.m at 4 °C	22 µm	200	200
18	20 mM ammonium formate in ultrapure water with 0.01% formic acid	4,4	2.1	2x 15min; 13000 r.p.m at 4 °C	22 µm	200	100



**DESENVOLVIMENTO DE UM MÉTODO POR CROMATOGRAFIA  
LÍQUIDA ACOPLADA A DETECÇÃO UV/ FLUORESCÊNCIA PARA A  
QUANTIFICAÇÃO DE METABOLITOS DA VIA QUINURENINÉRGICA  
EM PACIENTES COM INSUFICIÊNCIA CARDÍACA**

Ana Sousa<sup>1</sup>, Bruno Peixoto <sup>1,2</sup>, Pedro Pimenta<sup>1</sup>, Aurora Andrade<sup>3</sup>, Virgínia Gonçalves<sup>1</sup>, Patrícia Silva<sup>3</sup>, Sandra Leal<sup>1,2</sup>, Cláudia Ribeiro<sup>1,4</sup>

<sup>1</sup>CESPU, Instituto de Investigação e Formação Avançada em Ciências e Tecnologias da Saúde, Rua Central de Gandra, 1317, 4585-116 Gandra PRD, Portugal

<sup>2</sup>Centro de Investigação em Tecnologias e Sistemas de Informação em Saúde (CINTESIS). Porto/Portugal

<sup>3</sup>Departamento Clínico de Cardiologia do Centro Hospitalar do Tâmega e Sousa EPE. Penafiel/Portugal

<sup>4</sup>Centro Interdisciplinar de Investigação Marinha e Ambiental (CIIMAR), Universidade do Porto, Edifício do Terminal de Cruzeiros do Porto de Leixões, Av. General Norton de Matos s/n, 4050-208 Matosinhos, Portugal

**Introdução:** O triptofano é um aminoácido essencial que participa ativamente em diversos processos biológicos. Da sua metabolização pela via das quinureninas resultam vários metabolitos incluindo a quinurenina e o ácido quinurénico com atividades relevantes a nível cardíaco e neuronal [1]. Em condições fisiológicas normais existe um equilíbrio entre a concentração de quinurenina e de ácido quinurénico. No entanto, em doenças crónicas tais como doenças cardiovasculares e neurológicas tem-se verificado um aumento dos níveis séricos destes dois metabolitos [2].

**Objetivo:** Desenvolvimento e validação de um método por cromatografia líquida com deteção UV/fluorescência para quantificação do triptofano e dos seus metabolitos obtidos pela via quinureninérgica (quinurenina e ácido quinurénico) em amostras de urina de pacientes com insuficiência cardíaca.

**Resultados:** Para a otimização da separação do triptofano, ácido quinurénico, quinurenina e 3-nitro-tirosina (padrão interno) foi selecionada uma coluna de fase reversa: Luna PFP (2) 150 x 4,6 mm, 100Å, 3µm. Vários parâmetros foram testados, nomeadamente composição da fase móvel, fluxo e temperatura do forno de coluna. As melhores condições foram obtidas com uma solução de formato de amónia 20mM a pH 4,4 (ajustado com ácido fórmico) e acetonitrilo em modo isocrático, fluxo de 0,7 mL/min. A quinurenina, ácido quinurénico e 3-nitro-tirosina foram analisados por UV (comprimento de onda de 250 nm) e o triptofano foi analisado por fluorescência (comprimento de onda de excitação e emissão de 280 e 348 nm, respetivamente) e temperatura do forno de coluna a 25°C. Nestas condições foi possível obter a separação de todos os compostos em menos de 20 minutos. Foram também otimizadas as condições de extração dos destes compostos em amostras de urina. Nas condições otimizadas não foi verificada a presença de interferentes nos tempos de retenção dos compostos e foi possível obter uma recuperação superior a 47%.

**Conclusões:** A metodologia analítica desenvolvida será validada de acordo com guias internacionais e utilizada para a quantificação destes compostos em amostras de urina de pacientes com insuficiência cardíaca. A aplicação desta metodologia permitirá um melhor controlo do processo inflamatório sistémico dos pacientes e potenciar a procura de novos alvos terapêuticos.

Agradecimentos: Trabalho financiado pelo projeto Bineuro-CESPU-2016.

[1] Schwarcz R, Bruno JP, Muchowski PJ, Wu H-Q. Kynurenines in the mammalian brain: when physiology meets pathology. *Nat Rev Neurosci*:465–77, 2012.

[2] Rebnord EW, Strand E, Midttun Ø, Svingen GFT, Christensen MHE, Ueland PM, et al. The kynurenine:tryptophan ratio as a predictor of incident type 2 diabetes mellitus in individuals with coronary artery disease. *Diabetologia*: 1712–21, 2017.

### **Keypoints:**

Da metabolização do triptofano pela via quinureninérgica resultam a quinurenina e o ácido quinurénico que são afetados pelo estado inflamatório.

Doentes com insuficiência cardíaca têm um estado inflamatório que conduz a um aumento da degradação do triptofano.

A quantificação do triptofano e dos seus metabolitos é fundamental para compreender o estado bioquímico associado às doenças cardiovasculares.

# Desenvolvimento de um Método por Cromatografia Líquida Acoplada a Detecção UV/ Fluorescência para a Quantificação de Metabolitos da Via Quinureninérica em Pacientes com Insuficiência Cardíaca



Ana Sousa<sup>1</sup>, Bruno Peixoto<sup>1,2</sup>, Pedro Pimenta<sup>1</sup>, Aurora Andrade<sup>3</sup>, Virginia Gonçalves<sup>1</sup>, Patricia Silva<sup>3</sup>, Sandra Leal<sup>1,2</sup>, Cláudia Ribeiro<sup>1,4</sup>

<sup>1</sup>CESPU Instituto de Investigação e Formação Avançada em Ciências e Tecnologias de Saúde, Rua Central de Góndalo, 1317, 4905-116 Góndalo EPE, Portugal  
<sup>2</sup>Centro de Investigação em Tecnologias e Sistemas de Informação em Saúde (CITESES), Porto, Portugal  
<sup>3</sup>Departamento Clínico de Cardiologia do Centro Hospitalar do Tago e Sousa EPE, Beja, Portugal  
<sup>4</sup>Centro Interdisciplinar de Investigação Médica e Analítica (CIMIA), Universidade do Porto, Edifício de Tecnologia e Ciências do Porto de Saúde, Av General Dantas de Matos nº1, 4050-205 Matosinhos, Portugal



## INTRODUÇÃO

O triptofano é um aminoácido essencial que é metabolizado pela via das quinureninas (fig. 1), resultando vários compostos em amostras de urina nomeadamente a composição e metabolitos com atividade em diversos processos biológicos [1]. Existe associação entre doenças cardiovasculares e alteração dos níveis séricos dos metabolitos de triptofano (fig.2).



FIGURA 1. Via quinureninica.

FIGURA 2. Metabolitos do triptofano no soro de pacientes com insuficiência cardíaca.

## OBJETIVO

Desenvolver e validar um método por cromatografia líquida acoplada a deteção UV/fluorescência (LC-UV/FD) para análise do metabolismo do triptofano em pacientes com insuficiência cardíaca.

## MATERIAIS E MÉTODOS

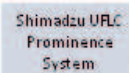
### 1. Preparação da amostra:



FIGURA 3. Esquematização do procedimento de preparação de amostra de urina.

### 2. Instrumentação:

Inte rface	- CBM-004
Bomba	- LC5040
Autoinjetor	- SIL2040C
Detetor UV/FD	- RF10AXL - SPD-004
Coluna	- Luna PFP (2)U70 4.6 mm 100Å 8µm
Forma de coluna	- CTC-004C
Condições cromatográficas	- 70°C, 900 nL a 0,7 mL/min - Fase móvel: 20 mM formiato amónio, pH 4,4; acetonitrilo: etanol



## RESULTADOS

Foram optimizadas as condições para a separação de todos os compostos em amostras de urina nomeadamente a composição e metabolitos com atividade em diversos processos biológicos [1]. Na fig.4 estão representados os cromatogramas da separação do triptofano (A) utilizando o detetor de FD e da quinurenina (B), L-nitrotirosina (C) e do ácido quinurenico (D) utilizando o detetor de UV.

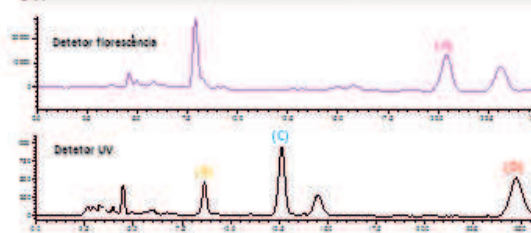


FIGURA 4. Cromatogramas de separação do triptofano (A) e da quinurenina (B) e amostras de urina (C) e do ácido quinurenico (D) utilizando o detetor de UV.

O método foi validado segundo as normas da Agência Europeia do medicamento (EMA)(2).

- Limite de quantificação (LQ)
- Exatidão
- Precisão
- Linearidade
- Recuperação

Na fig. 5 estão representadas as curvas de calibração para o triptofano (A), quinurenina (B) e ácido quinurenico (C).

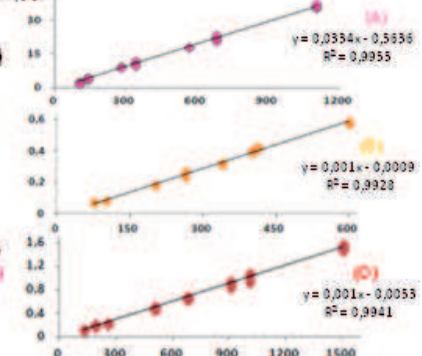


FIGURA 5. Curvas de calibração do triptofano (A), quinurenina (B) e ácido quinurenico (C) obtidas a partir de urina.

## CONCLUSÃO

O presente método foi aplicado para quantificação dos compostos em amostras de urina de pacientes com doença cardíaca. A quantificação do triptofano e dos seus metabolitos é fundamental para compreender o estado bioquímico associado às doenças cardiovasculares.

## REFERÊNCIAS

- (1) Wang Q, et al. Front Biosci Landmark Ed. 2015;20:1126-1148.
- (2) Liu H, et al. Am J Epidemiol. 2016; 183(4):246-252.
- (3) European Medicine Agency (EMA). Guide to the preparation of method validation.

Agradecimentos: Trabalho financiado pelo CESPU-Cooperativa de Ensino Superior Politécnico e Universitário no âmbito do projeto BineuroCESPUC048.